ISSN 2218-6255 (online)

World Journal of *Respirology*

World J Respirol 2019 January 27; 9(2): 8-29

Published by Baishideng Publishing Group Inc

WJR

World Journal of Respirology

Contents

Irregular Volume 9 Number 2 January 27, 2019

REVIEW

Contents

World Journal of Respirology

Volume 9 Number 2 January 27, 2019

ABOUT COVER

Editorial Board Member of *World Journal of Respirology*, Bo Deng, MD, PhD, Associate Professor, Thoracic Surgery Department, Institute of Surgery Research, Daping Hospital, Third Military Medical University, Chongqing 400042, China

AIMS AND SCOPE

World Journal of Respirology (*World J Respirol*, *WJR*, online ISSN 2218-6255, DOI: 10.5320) is a peer-reviewed open access academic journal that aims to guide clinical practice and improve diagnostic and therapeutic skills of clinicians.

WJR covers topics concerning respiratory physiology, respiratory endoscopy, respiratory system tumors, chronic obstructive pulmonary disease, bronchial asthma, respiratory infections, critical respiratory illness, sleep-related respiratory disorders, interstitial lung disease, *etc*. The following aspects are covered: Clinical diagnosis, laboratory diagnosis, differential diagnosis, imaging tests, pathological diagnosis, molecular biological diagnosis, *etc*.

We encourage authors to submit their manuscripts to *WJR*. We will give priority to manuscripts that are supported by major national and international foundations and those that are of great basic and clinical significance.

INDEXING/ABSTRACTING

World Journal of Respirology is now abstracted and indexed in China National Knowledge Infrastructure (CNKI), China Science and Technology Journal Database (CSTJ), and Superstar Journals Database.

RESPONSIBLE EDITORS FOR THIS ISSUE

Responsible Electronic Editor: *Yan-Liang Zhang* **Proofing Editorial Office Director:** *Ya-Juan Ma*

NAME OF JOURNAL
World Journal of Respirology

ISSN
ISSN 2218-6255 (online)

LAUNCH DATE
December 30, 2011

FREQUENCY
Irregular

EDITORIAL OFFICE
Ya-Juan Ma, Director

PUBLICATION DATE
January 27, 2019

INSTRUCTIONS TO AUTHORS
https://www.wjgnet.com/bpg/gerinfo/204

GUIDELINES FOR ETHICS DOCUMENTS
https://www.wjgnet.com/bpg/GerInfo/287

GUIDELINES FOR NON-NATIVE SPEAKERS OF ENGLISH
https://www.wjgnet.com/bpg/gerinfo/240

PUBLICATION MISCONDUCT
https://www.wjgnet.com/bpg/gerinfo/208

ARTICLE PROCESSING CHARGE
https://www.wjgnet.com/bpg/gerinfo/242

STEPS FOR SUBMITTING MANUSCRIPTS
https://www.wjgnet.com/bpg/GerInfo/239

ONLINE SUBMISSION
https://www.f6publishing.com

World Journal of Respirology

Submit a Manuscript: https://www.f6publishing.com

World J Respirol 2019 January 27; 9(2): 8-29

DOI: 10.5320/wjr.v9.i2.8

ISSN 2218-6255 (online)

REVIEW

Anatomical backgrounds on gas exchange parameters in the lung

Kazuhiro Yamaguchi, Takao Tsuji, Kazutetsu Aoshiba, Hiroyuki Nakamura, Shinji Abe

ORCID number: Kazuhiro Yamaguchi (0000-0002-9135-2161); Takao Tsuji (0000-0002-0501-3543); Kazutetsu Aoshiba (0000-0002-9490-9754); Hiroyuki Nakamura (0000-0003-2821-971X); Shinji Abe (0000-0003-0949-4601).

Author contributions: All authors contributed to the conception and design of the study; they contributed acquisition, analysis, and interpretation of the data; they expressed the final approval of the version of the article.

Conflict-of-interest statement: The authors have no conflict of interest to declare; there were no supportive foundations to the present study.

Manuscript source: Invited manuscript

Received: September 3, 2018
Peer-review started: September 3, 2018
First decision: October 26, 2018
Revised: November 11, 2018
Accepted: December 16, 2018
Article in press: December 17, 2018

Kazuhiro Yamaguchi, Takao Tsuji, Shinji Abe, Department of Respiratory Medicine, Tokyo Medical University, Tokyo 160-0023, Japan

Kazutetsu Aoshiba, Hiroyuki Nakamura, Department of Respiratory Medicine, Tokyo Medical University, Ibaraki Medical Center, Ibaraki 300-0395, Japan

Corresponding author: Kazuhiro Yamaguchi, FCCP, MD, PhD, Guest Professor, Department of Respiratory Medicine, Tokyo Medical University, 6-7-1 Nishi-Shinjuku, Shinjuku-ku, Tokyo 160-0023, Japan. yamaguc@sirius.ocn.ne.jp
Telephone: 81-3-34215402
Fax: +81-3-34215402

Abstract

Many problems regarding structure-function relationships have remained unsolved in the field of respiratory physiology. In the present review, we highlighted these uncertain issues from a variety of anatomical and physiological viewpoints. Model A of Weibel in which dichotomously branching airways are incorporated should be used for analyzing gas mixing in conducting and acinar airways. Acinus of Loeschcke is taken as an anatomical gas-exchange unit. Although it is difficult to define functional gas-exchange unit in a way entirely consistent with anatomical structures, acinus of Aschoff may serve as a functional gas-exchange unit in a first approximation. Based on anatomical and physiological perspectives, the multiple inert-gas elimination technique is thought to be highly effective for predicting ventilation-perfusion heterogeneity between acini of Aschoff under steady-state condition. Changes in effective alveolar P_{O2}, the most important parameter in classical gas-exchange theory, are coherent with those in mixed alveolar P_{O2} decided from the multiple inert-gas elimination technique. Therefore, effective alveolar-arterial P_{O2} difference is considered useful for assessing gas-exchange abnormalities in lung periphery. However, one should be aware that although alveolar-arterial P_{O2} difference sensitively detects moderately low ventilation-perfusion regions causing hypoxemia, it is insensitive to abnormal gas exchange evoked by very low and high ventilation-perfusion regions. Pulmonary diffusing capacity for CO (D_{LCO}) and the value corrected for alveolar volume (V_{AV}), *i.e.*, D_{LCO}/V_{AV} (K_{CO}), are thought to be crucial for diagnosing alveolar-wall damages. D_{LCO}-related parameters have higher sensitivity to detecting abnormalities in pulmonary microcirculation than those in the alveolocapillary membrane. We would like to recommend four categories derived from combining behaviors of D_{LCO} with those of K_{CO} for differential diagnosis on anatomically morbid states in alveolar walls: type-1 abnormality defined by decrease in both D_{LCO} and K_{CO}; type-2 abnormality by decrease in D_{LCO} but increase in K_{CO}; type-3 abnormality by decrease in D_{LCO} but restricted rise in K_{CO}; and type-4 abnormality by increase in both D_{LCO} and K_{CO}.

Published online: January 27, 2019

Key words: Secondary lobule of miller; Acinus of Loeschcke; Acinus of Aschoff; Convection; Gas-phase diffusion (stratification); Aqueous-phase diffusion; Ventilation-perfusion heterogeneity

Core tip: The anatomical gas-exchange unit is organized into the acinus of Loeschcke, while the functional gas-exchange unit is given by the acinus of Aschoff. The ventilation-perfusion distribution in acinar regions is representatively predicted from the inert-gas elimination technique. The effective alveolar-arterial P_{O2} difference plays a vital role in detecting moderately low ventilation-perfusion regions eliciting hypoxemia but not very low and high ventilation-perfusion regions. Pulmonary diffusing capacity for CO and the value corrected for alveolar volume estimate the impediment of alveolar walls and are more sensitive to detecting the abnormality of pulmonary microcirculation than that of alveolocapillary membrane.

Citation: Yamaguchi K, Tsuji T, Aoshiba K, Nakamura H, Abe S. Anatomical backgrounds on gas exchange parameters in the lung. *World J Respirol* 2019; 9(2): 8-29
URL: https://www.wjgnet.com/2218-6255/full/v9/i2/8.htm
DOI: https://dx.doi.org/10.5320/wjr.v9.i2.8

INTRODUCTION

The morphological and physiological aspects of normal and diseased lungs were most actively studied in the era of the 20th century from the 1950's to the 1980's. The morphological and physiological approaches are both equally important for raising the quality of basic science and of clinical medicine targeting the human lung. Although the lung morphology and the respiratory physiology have evolved in parallel, it is hard to say that the efforts to unite them in a variety of directions by morphologists, physiologists, and clinicians, *i.e.*, the establishment of structure-function relationships, were successful enough. It is of clinical value to understand the anatomical basis of various functional parameters during pathophysiological decision-making in patients with various types of lung disease. Based on these historical facts, we try to shed light on the elucidation of anatomical backgrounds of various functional parameters that have been used for estimating gas maxing in conducting airways and gas exchange in the lung periphery. To accomplish this purpose, the following five matters were comprehensively addressed in the present review: (1) What is the appropriate anatomical design for understanding gas mixing in conducting airways and gas exchange in lung periphery? (2) Aspects of convective and diffusive gas mixing along peripheral airways in a lung model in which dichotomously branching airways are certainly considered. (3) Is the ventilation-perfusion (V_A/Q) distribution in the lung, which is quantitated in terms of the multiple inert-gas elimination technique (MIGET), supported by the anatomical and physiological facts? (4) Is the effective alveolar-arterial P_{O2} difference ($AaDO_2$) estimated from the classical gas-exchange theory also supported by the anatomical and physiological facts? (5) What are the anatomical and physiological determinants on the pulmonary diffusing capacity for carbon monoxide (D_{LCO})?

Anatomical design for understanding gas mixing and gas exchange in the lung

Branching of conducting airways: The pattern of airway branching in a normal lung is best studied on resin or silicon rubber casts[1-8] (Figure 1). The lower conducting airways end in clusters that are surrounded by the fibrous connective tissue septa. The cluster is defined as the secondary lobule of Miller[9,10], which contains lobular (preterminal) bronchioles and terminal bronchioles that supply the gas to or from the acini of Loeschcke[10].

Although conducting airways are most often described as a symmetric tree that branches off by regular dichotomy, in which all pathways have exactly the same length and each generation of branching is composed of airways uniform in size[2,3,11], this type of model is in fundamental conflict with the anatomical facts[2,12,13]. A more realistic representation is a tree of irregular, asymmetric dichotomy, where the dimension of conjugate daughter branches differs from that of their parents. The

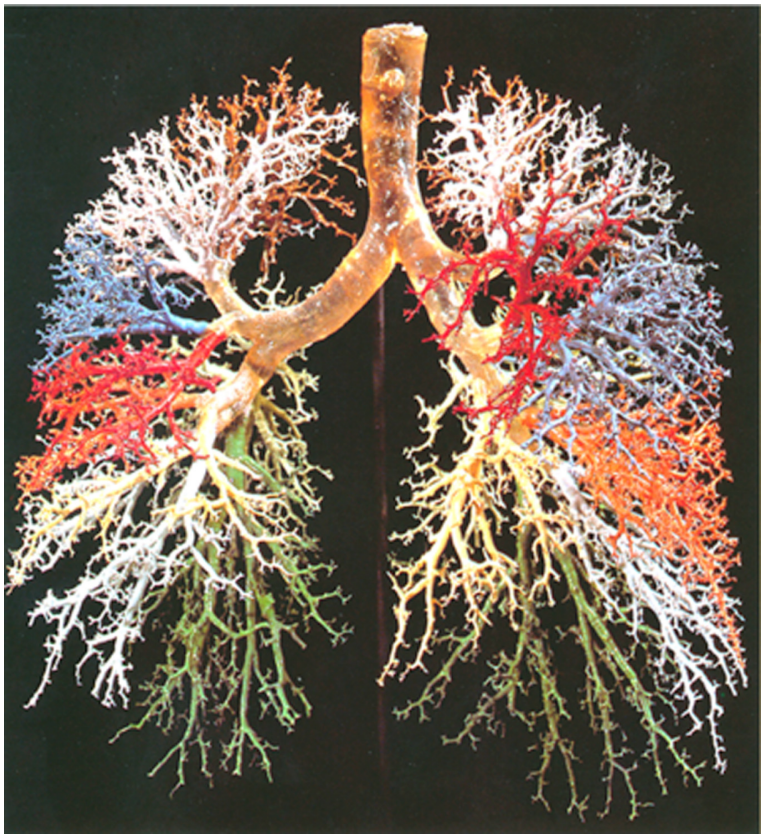

Figure 1 Resin cast of human lung. Complicated dichotomously branching tree of conducting airways is exhibited. Adopted from ref[1].

irregular dichotomy includes different branching angle and varied length-to-diameter ratio at a certain airway generation. Weibel[2,3] demonstrated that the pathway length in airways with 1.5-mm diameter varies between 1.5 mm and 11 mm, with the highest frequency at 3.5-4.0 mm. Similarly, airways of 2.0 mm in diameter (*i.e.*, small airways) are spread out between the 4th and 14th generations of the branching tree, with a maximum at the 8th generation. The valuable message emanating from the studies of Weibel is that although conducting airways are correctly modeled by an irregular, asymmetric dichotomous branching tree, the dimensional variation of airway diameters and path lengths assigned to each generation of the tree nearly follows the normal distribution, and this variation decreases as the generation progresses. Based on these findings, a simple design called "model A of Weibel"[2,3] or "typical path lung model"[4,5,14] has been developed. This model assumes that in an initial approximation, the asymmetric branching tree can be replaced by the symmetric branching tree using the mean (representative) value estimated from the normal distribution of airway diameters as well as that of path lengths at a given generation (Figure 2), which results in that one can assess gas mixing in the conducting airways with asymmetric branches from the model A of Weibel with simple geometry.

Anatomical definition of lobule and acinus: Different terms have been used for defining the lobule and the acinus throughout several decades. In 1947, Miller proposed the anatomical concept that is valuable for understanding the secondary and primary lobules[9]. As described above, the secondary lobule of Miller is the unit supplied by a lobular bronchiole having a diameter of about 1.0 mm (corresponding to the 12th generation) and surrounded by the fibrous connective tissue septa (*i.e.*, the interlobular septa) (Figure 3). The size of secondary lobules of Miller varies from 1.0 cm to 2.5 cm, each of which is comprised of varying numbers of acini defined by Loeschcke, ranging from three to twenty-four depending on the region selected[15,16]. On the other hand, the primary lobule of Miller is expressed by the area governed by an alveolar duct. The secondary lobule proposed by Miller has various advantages from anatomical points of view. Therefore, unless otherwise specified, the simple term of "secondary lobule" is used in the sense of "secondary lobule of Miller" throughout the current review.

In 1958, based on the bronchogram of peripheral airways, Reid[17,18] presented a different definition with regard to the secondary lobule. The secondary lobule of Reid

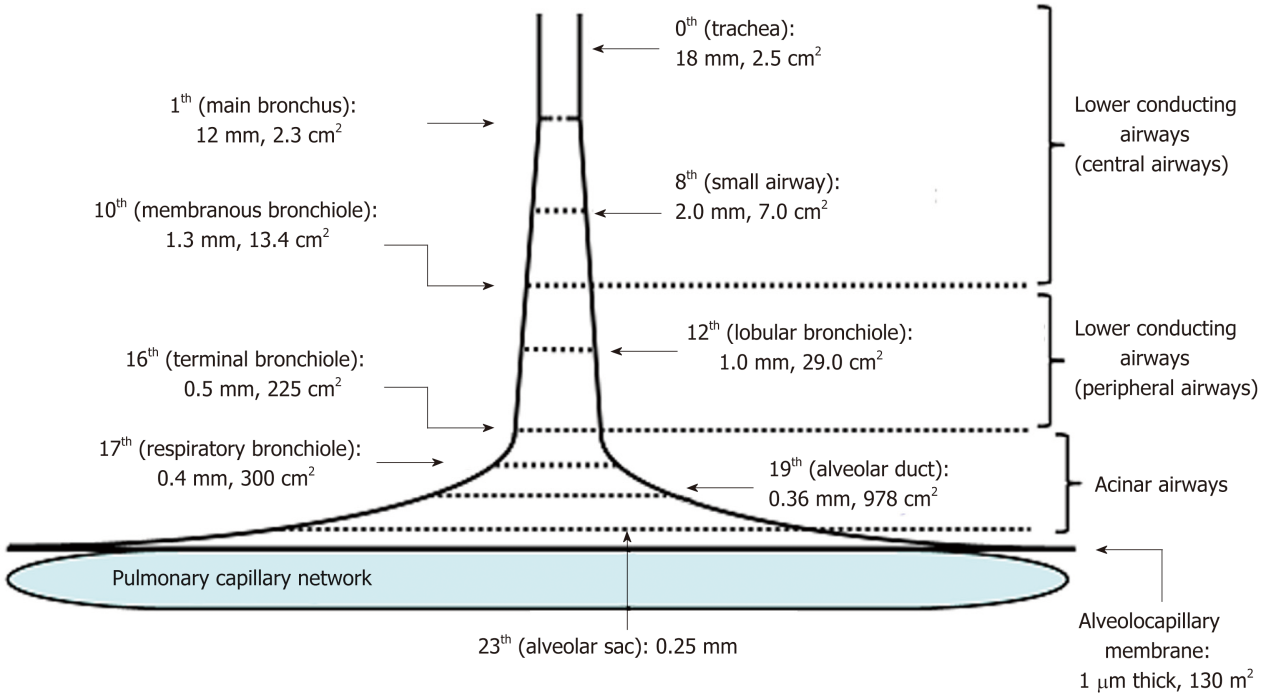

Figure 2 Schematic presentation of effective diameter and cross-sectional area along lower conducting airways and acinar airways (trumpet or thumbtack model). Generations of branching tree and diameter as well as cross-sectional area in each generation are obtained from model A of Weibel[2]. Lower conducting airways are classified into two routes; *i.e.*, central airways [generation from zero (trachea) to 9th] and peripheral airways (generation from 10th to 16th, in which 16th generation corresponds to terminal bronchiole). Peripheral airways are characterized by membrane bronchioles, whereas small airways are defined by their diameters of less than 2.0 mm originating in the 8th generation. Airways from the 17th generation (respiratory bronchiole) to the 23th generation (alveolar sac) are not included in peripheral airways. Instead, they are defined as acinar (alveolated) airways (acinus indicates that defined by Loeschcke). This is because acinar airways function by carrying gas and exchanging gas. Alveolar sacs end in alveoli formed by alveolar walls containing alveolocapillary membranes and capillary networks. Thickness of the alveolocapillary membrane is about 1.0 μm and total cross-sectional area of the alveolocapillary membrane and capillary network is about 130 m^2.

is the unit formed by the structure distal to any bronchiole having a mm-branching pattern. The size of the secondary lobule of Reid is fairly constant (approximately 1.0 cm) in comparison with that of Miller and contains three to five acini of Loeschcke. The Reid's definition is more useful when interpreting the bronchogram.

The acinus of Loeschcke is the unit distal to a terminal bronchiole (Figure 3), in which all alveolated airways engage in gas exchange. The size of the acinus of Loeschcke averages 7 mm to 10 mm in diameter and roughly 80000 acini configure the lung. An acinus contains alveoli ranging from 3000 to 4000[8,19], resulting in the lung consisting of 300-million alveoli.

The acinus of Aschoff is defined as the area supplied by a first-order respiratory bronchiole (Figure 3), the size of which is half of the acinus of Loeschcke[20]. All alveolated airways in the acinus of Aschoff participate in gas exchange. The acinus of Loeschcke is important when defining the anatomical gas-exchange unit, while the acinus of Aschoff is important when the functional gas exchange is defined.

Similar to conducting airways, intra-acinar, alveolated airways (respiratory bronchioles, alveolar ducts, and alveolar sacs) also show irregular dichotomous branching over an average of nine generations, terminating at between the 6th to 12th generations[8,21,22]. Large acini have more generations and smaller acini have correspondingly fewer. Although the issue of whether the variation of airway diameters and path lengths of each generation in the acinus (Loeschcke or Aschoff) follows the normal distribution has not been reliably concluded, Weibel and colleagues[2,3,8] presumed that the geometrically-simple model A of Weibel could be applied for integrating the branches of conducting airways and acinar airways. The features of model A of Weibel (Figure 2), which is also called the "trumpet model" or "thumbtack model", are summarized as follows[2,23,24]: (1) the model consists of the average number of generations over which the airways must terminate in the alveolar sacs corresponding to the 23th generation; (2) the 16th generation defines the terminal bronchiole; (3) the 17th-22th generations correspond to the acinar airways, including the respiratory bronchioles and alveolar ducts; and (4) the number of airways in a particular generation increases tremendously as the generation increases, leading to the exponential increase in the generation-specific total cross-sectional area. Weibel[2]

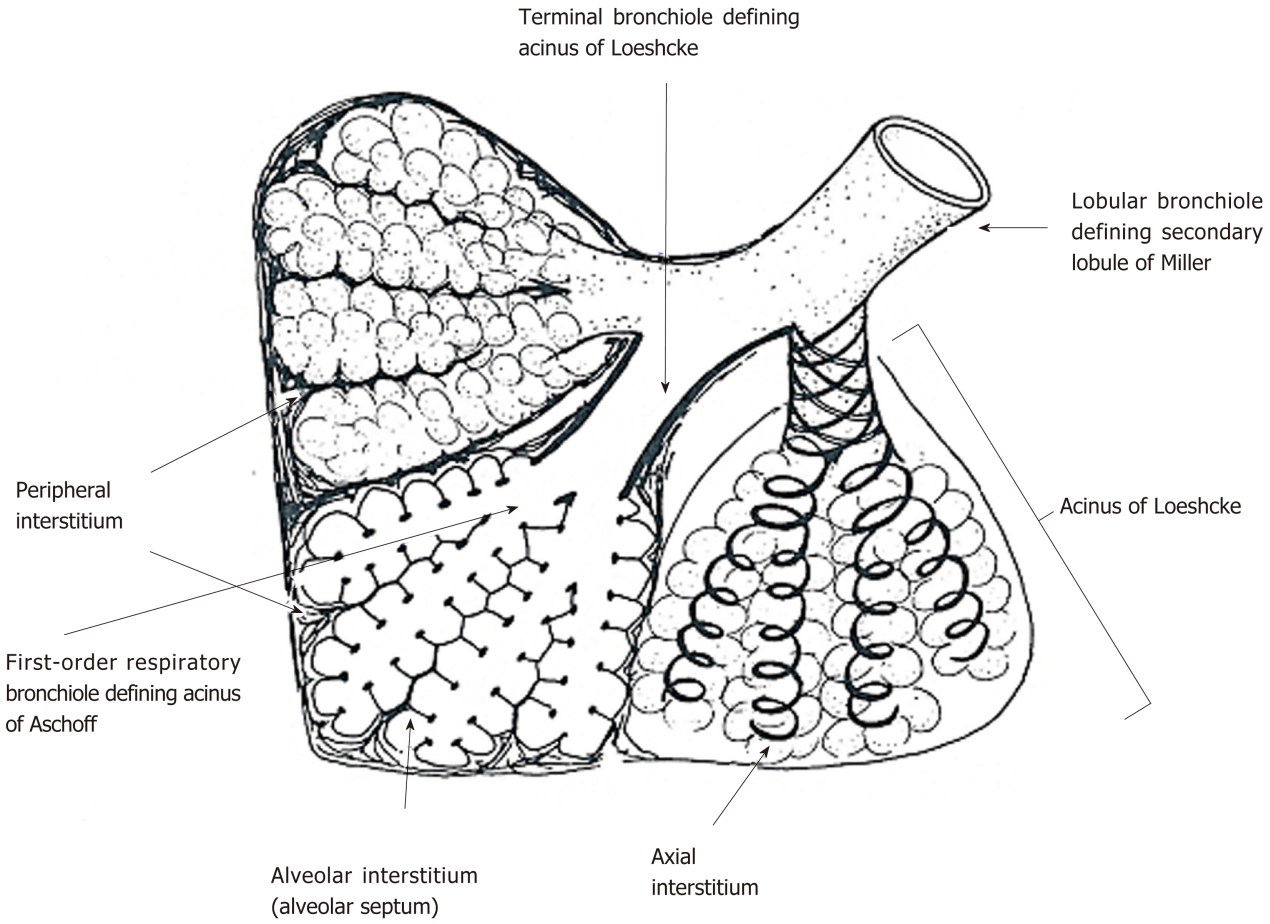

Figure 3 Secondary lobule and acinus. Secondary lobule of Miller is defined by the area supplied by a lobular bronchiole while the acinus of Loeschcke is defined by the area supplied by a terminal bronchiole. Acinus of Aschoff is the area supplied by a first-order respiratory bronchiole. Secondary lobule of Miller is surrounded by fibrous connective tissue forming interlobular septum. In acini of Loeschcke and Aschoff, there are three important interstitial tissues, including peripheral interstitium, alveolar interstitium forming alveolar septum, and axial interstitium spirally surrounding airways, which begins at the alveolar duct extending to the hilum. Axial interstitium and alveolar interstitium are joined via intra-parenchymal interstitium and all interstitial tissues are in a serial linkage. Modified from ref[2].

demonstrated that the average diameter of terminal bronchiole, respiratory bronchiole, or alveolar duct is 0.50 mm, 0.39 mm, and 0.33 mm, respectively, while the average total cross-sectional area of these airways is 230 cm^2, 420 cm^2, and 2630 cm^2 (equal to 0.263 m^2), respectively. The total cross-sectional area including all alveoli amounts to about 130 m^2 in association with the harmonic mean thickness of alveolocapillary membrane of 1.1 μm[25].

Anatomical aspects of collateral ventilation: Three pathways exist for collateral ventilation in the acinus, *i.e.*, alveolar pores (pores of Kohn), channels of Lambert, and channels of Martin. Although the typical size of alveolar pores ranges from 2 μm to 30 μm, there have been many anatomical, physiological, and theoretical studies leading to the conclusion that the alveolar pores are not potent in air-filled lungs[26,27]. These studies indicate that the alveolar pores take no part in maintaining alveolar ventilation.

In 1955, Lambert[28] described accessory communications between bronchioles and alveoli in the normal human lung. The diameter of Lambert channels varies from 0 μm (practically closed) to 30 μm, and they are considered to serve as collateral ventilation to adjacent alveoli when airway obstruction occurs at the level of terminal bronchioles[27]. Supporting this consideration, the important role of Lambert channels was identified in patients with pneumoconiosis, in which a striking accumulation of macrophages was found in the Lambert channels and their adjacent alveoli[29].

In 1966, Martin[30] reported intra-acinar communications at the level of respiratory bronchioles or alveolar ducts in the canine lung. The Martin channels were found in human lungs as well[9,31]. As the Martin channels have sufficiently low resistance to gas flow, they act as the primary pathway for inducing collateral ventilation in the acinus[27]. Therefore, one can conceive that only the Martin channels but neither the alveolar pores nor the Lambert channels serve to equalize the distribution of alveolar

ventilation and the concentration of a certain gas in a particular acinus, though the extent of equalization elicited by collateral ventilation has not been conclusively quantified.

Definition of anatomical gas-exchange unit – importance of acinus of Loeschcke: The alveolus cannot be taken as a ventilation unit mostly because each alveolus is not independent of other alveoli. Two adjoining alveoli share the alveolar wall and each alveolus adjoins several alveoli, some of which are connected to different alveolar ducts. Furthermore, there are communications at the level of respiratory bronchioles or alveolar ducts (Martin channels). On the other hand, the acinus of Loeschcke can be taken as an anatomical ventilation unit because it is supplied only by a single conducting airway with no alveoli, *i.e.*, the terminal bronchiole (Figure 3).

There is a serious problem concerning a perfusion unit formed by the pulmonary microcirculation. The dense, intertwined capillary network embedded in the alveolar wall forms a continuum of blood flow that is not partitioned into independent perfusion units. This disproves that the gas-exchange unit is organized into an alveolus associated with a separated capillary network in the alveolar wall. The capillary network is supplied by the arteriole that penetrates into the acinus along the acinar airways and is drained into the venule in the acinar periphery. The distance between an arteriole and a venule is of an order between 0.5 mm and 1.0 mm[32], suggesting that the perfusion unit given by the area surrounded by an arteriole and a venule extends over several alveoli, but it does not cover the whole area of an acinus of Loeschcke whose size ranges from 7 mm to 10 mm[25]. These facts are in accord with the idea that the perfusion unit is not congruent with the ventilation unit so that it gives rise to difficulty in anatomically defining the gas-exchange unit in which the ventilation and perfusion units should be matched. However, König *et al*[33] found that the whole acinar region of Loeschcke is perfused almost homogeneously by colloid gold used as a plasma tracer even at rest, indicating that all capillary networks existing in the acinus of Loeschcke are connected to each other. Based on the study of König *et al*[33], we considered that the anatomical gas-exchange unit is organized approximately into the acinus of Loeschcke.

Convective and diffusive gas mixing in conducting and acinar airways

In addition to the convective mixing elicited by ventilation, the diffusive mixing plays an important role in maintaining gas transport along peripheral and acinar airways with large cross-sectional areas (Figure 2). Numerous mathematical attempts have been made to estimate the effect of convection, diffusion, or interactions of both on gas transport in conducting and acinar airways using a model with symmetrically or asymmetrically dichotomous branching of airways[24]. The term of convection is defined as a mass transport resulting from the unidirectional displacement of molecules included in a certain volume. Convective displacement is identical for all molecular species and is not different for gases with different diffusivity. This indicates that convection (laminar or turbulent flows) occurs along gradients of total pressure but not along those of partial pressure.

On the other hand, the term of diffusion is defined as a result from the random motion of molecules due to their thermal energies, depending on their concentration (partial pressure) gradients and diffusivity. Hence, a separation of two gases with different diffusivity occurs during gas transport when diffusive transport constitutes a main limiting process, whereas a separation of two gases is not investigated when gas transport is mainly limited by convection. Diffusive transport in airways and alveoli occurs in axial and radial directions; yet the mechanism of these two directions is the same. Furthermore, the coupling of convection and diffusion occurs under a condition where the contribution of convection and diffusion to gas transport is of similar magnitude, which may occur predominantly in peripheral airways at generations between the 8th and 12th[34]. The magnitude of convection-diffusion coupling under a condition of laminar or turbulent flow is estimated using the dispersion coefficient proposed by Taylor and others[35-38]. However, the Taylor dispersion has been identified to be insignificant for gas transport during normal breathing[39-43], leading to the conclusion that it is enough to introduce only the convection and diffusion (particularly, axial diffusion), but not the dispersion, as the basic mechanism when assessing the gas transport along conducting and acinar airways.

Introducing both convection and diffusion as the gas mixing mechanism into model A of Weibel that has a simple geometry with trumpet or thumbtack shape, several groups of investigators analyzed the time-dependent change in gas concentration profile of an insoluble gas that is not absorbed into the blood (*i.e.*, no gas exchange) along peripheral conducting airways and acinar airways during normal breathing[39,44-50]. Paiva[46] assumed: (1) no dispersion in airways; (2) no radial diffusion

in airways; (3) no axial diffusion in alveolar regions; (4) no convective flow in alveolar regions (*i.e.*, alveoli simply act as a sink for diluting a gas during inspiration while as a reservoir for expelling a gas during expiration); and (5) no collateral ventilation in acinar regions. As the theoretical calculation by Paiva[46] was made under a situation where the tidal volume was set at 500 mL and the functional residual capacity at 3000 mL (*i.e.*, the representative lung volume during normal breathing), the end-inspiratory gas concentration in the alveolar region is reduced to 17% of that at the beginning of inspiration. Paiva[46] analyzed gas mixing kinetics along airways constituting the last 13th generations, which correspond closely to the secondary lobule of Miller (Figures 2 and 3). The results emphasized by Paiva[46] are summarized below (Figure 4):

(1) On inspiration, the front of a gas, which is expressed by the axial distance at which the concentration of a gas is reduced to 50% of the value at the beginning of inspiration, lags appreciably behind the front of tidal volume. The front of tidal volume attains to the 22th generation of airways (*i.e.*, the alveolar duct), whereas the front of a gas stays at the 17th generation (*i.e.*, the first-order respiratory bronchiole defining the acinus of Aschoff). The gas front is practically stationary, suggesting that the convective advancement of a gas into the periphery is counterbalanced by the diffusion-elicited proximal retreat of a gas. The volume from the airway entrance to the gas front is about 150 mL, which corresponds to the common dead space volume conceptualized in the classical gas-exchange theory. This indicates that the classical, common dead space can be defined as the inspiratory volume decided by the gas front, but not by the front of tidal volume. Furthermore, the classical gas-exchange theory assumes that the front of common dead space has a sharp, all-or-nothing transition boundary as if it is formed only by the ventilation-induced convective flow, implying that the effect of diffusion is converted to the equivalent effect of convection. The region distal to the boundary is the alveolar region in which gas exchange takes place. The definition of dead space specified by Paiva[46] issues an important message as to the way of how to define the functional gas exchange unit in the steady-state V_A/Q analysis and classical gas exchange theory, both of which will be argued in the following sections.

(2) On expiration, all intrapulmonary concentration gradients of a gas are rapidly faded out, which is mainly caused by the thoracic shrinkage-induced convective flow during expiration. The diffusive process in acinar gas phase imposes a negative impact on gas transport in an early stage, but not in a later stage, of expiration. The aforementioned findings during one respiratory cycle indicate that the stratification (*i.e.*, the concentration gradient of a gas due to diffusion) is evident along acinar airways during inspiration but is minimal during expiration. Differing from inspiratory phase, the common dead space formed by the non-alveolated, conducting airways exerts nearly no impact on gas transport in conducting airways during expiratory phase. Instead, the common dead space literally functions as a simple reservoir for diluting the gas expelled from all alveolar regions during expiration.

Quantification of continuous distribution of V_A/Q

Definition of functional gas-exchange unit – importance of acinus of Aschoff: In general, the continuous distribution of V_A/Q in the lung has been quantitated by means of the MIGET. The most important matter in the MIGET is how to define the functional gas-exchange unit in which concentration of a gas should show uniform value. Although the acinus of Loeschcke approximates the anatomical gas-exchange unit, it is uncertain as to the issue of whether the acinus of Loeschcke concurrently serves as the functional gas-exchange unit. In the acinus of Loeschcke, an alveolus adjoins several alveoli and there are communications at the level of respiratory bronchioles or alveolar ducts (Martin channels), both of which tend to equalize gas-concentration difference over the acinus of Loeschcke. However, the point of whether the equalization of gas concentration in the acinus of Loeschcke is complete has not been confirmed. Therefore, it may be fraught with the problem to blindly adopt the acinus of Loeschcke as the functional gas-exchange unit.

In fact, Paiva *et al*[51] suggested that the regions distal to the alveolar duct, which correspond to the primary lobules of Miller, have different gas concentrations at the end of inspiration after a single-breath of a non-absorbable gas. However, they[51] also demonstrated that the gas-concentration difference between respective primary lobules of Miller formed during inspiration diminishes rapidly during expiration. Furthermore, caution should be paid to the fact that Paiva *et al*[51] disregarded the effect of Martin channels-induced collateral ventilation on gas-concentration equalization between the primary lobules of Miller. If the collateral ventilation-elicited equalization effect is taken into consideration, the gas-concentration difference between the primary lobules of Miller is expected to become much smaller. The importance of the acinus of Aschoff given by the region distal to the first-order

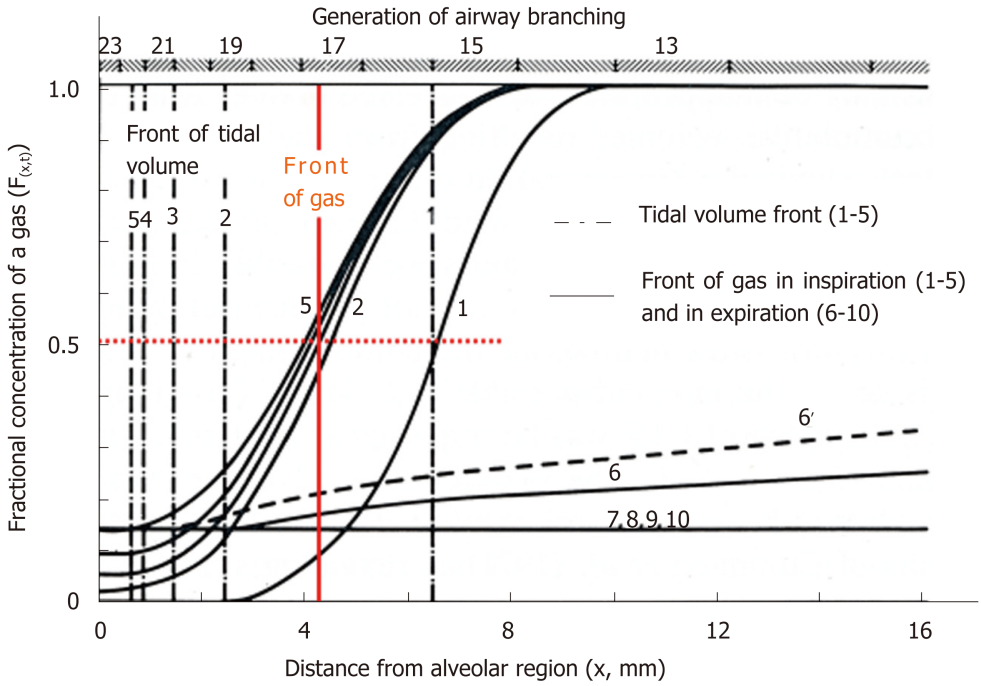

Figure 4 Concentration profiles along peripheral conducting airways and acinar airways during the respiratory cycle in thumbtack model. Upper abscissa: generation of airway branching defined in model A of Weibel. Lower abscissa: axial distance from alveolar region. Ordinate: fractional concentration of the test gas. 100% O_2 is inhaled (single breath) into and then exhaled from initially O_2-free lung with constant flow (tidal volume: 500 mL) and constant lung volume (functional residual capacity: 3000 mL). O_2 is assumed to not be absorbed into capillary blood (*i.e.*, no gas exchange). Solid curves (black) indicate concentration profiles at successive equally timed periods during inspiration (1-5) and expiration (6-10). Dashed dotted lines (1-5) are tidal volume fronts (*i.e.*, concentration fronts of non-diffusible tracer gas) during inspiration. Dashed line (6') is a concentration profile calculated on assumption of no axial diffusion during expiratory phase corresponding to time point of solid line (6). Red solid line denotes "imaginary" boundary between common dead space and alveolar region conceptualized in classical gas-exchange theory. Boundary is defined by stationary gas front converting diffusional effect into equivalent convectional effect, which is formed at entrance of acinus of Aschoff (17th generation of branching tree). See text for detailed explanation. Modified from ref[46].

respiratory bronchiole as the functional gas-exchange unit was implicitly indicated by Paiva[46]. He showed that the "imaginary" boundary separating the alveolar gas-exchange region from the dead space exists in the vicinity of the first-order respiratory bronchiole corresponding to the entrance of the acinus of Aschoff (Figures 3 and 4). As such, the study of Paiva[46] suggests that the functional gas-exchange unit under a steady-state condition is close to the anatomically defined acinus of Aschoff. This is because the size of the acinus of Aschoff is about half of the acinus of Loeschcke such that the gas-concentration variation, if any, is much smaller between the acini of Aschoff than that between the acini of Loeschcke. This results in that the acinus of Aschoff satisfies the essential requirement for the functional gas-exchange unit, namely the uniformity of gas concentration over the unit, more precisely than the acinus of Loeschcke does. Hence, we considered that the functional gas-exchange unit should be defined by the acinus of Aschoff whose area is smaller than that of the anatomical gas-exchange unit formed by the acinus of Loeschcke, leading to the conclusion that the MIGET argued in this section should be thought to predict the V_A/Q heterogeneity between the acini of Aschoff.

Basic rationale for determining V_A/Q distribution: Under a steady-state condition in which there is no change in the partial pressure of a gas (P) against the elapsed time (t) at any portion of the lung (*i.e.*, $\Delta P/\Delta t$ = zero), the partial pressure of an inert gas in gas phase (P_A) and that in blood phase (P_c) of a given functional gas-exchange unit are described by the simple equation in accordance with the law of mass balance[19,52-54].

$P_A/P_v = P_c/P_v = \lambda/(\lambda + V_A/Q)$ ····· eq. 1

Where P_v denotes the partial pressure of a given inert gas in mixed venous blood, whereas λ is the blood-gas partition coefficient of a gas, which is decided by its blood solubility (α)[19,55]. The eq. 1 is approved only in a condition where the inspired air does not contain any trace of an inert gas. This holds true when an inert gas is infused through the peripheral vein but not when it is inhaled through the mouth. The eq.1 implies that the partial pressure of an inert gas in the functional gas-exchange unit is simply determined by the ratio of convective flow of ventilation (V_A) and that of perfusion (Q) distributed to each functional gas-exchange unit. There are many

physiological assumptions that should be addressed for the establishment of eq. 1[19,54,56-59]. They are listed below.

(1) The functional gas-exchange unit is in a steady state such that the net transfer rate of an inert gas from capillary blood to alveoli in the functional gas-exchange unit exactly equals the net rate of elimination through expiration. Thus, the amount of an inert gas stored in blood, lung tissue, or alveoli is constant. The condition in which the MIGET is applied meets the steady-state definition.

(2) The tidal nature of ventilation is ignored. Namely, the rebreathing of a gas fulfilling the common dead space in previous expiration is not considered. The MIGET assumed the specific, personal dead space connecting to the individual functional gas-exchange unit. Therefore, in the next inspiration, each functional gas-exchange unit inhales the gas from each personal dead space that has the same gas composition as that expelled from each functional gas-exchange unit in the previous expiration. This assumption is highly dissociated from the anatomical and physiological facts. However, the volume of common dead space configured by upper and lower conducting airways amounts to 150 mL, which corresponds to only 5% of the lung volume represented by the functional residual capacity (3000 mL), suggesting that the gas contained in the common dead space is diluted largely when it reaches the gas-exchange units at an early stage of the next inspiration. Furthermore, the inspiratory tidal volume is 500 mL so that after inhaling the gas remaining in the dead space (150 mL), which is the averaged mixed alveolar gas exhaled from all functional gas-exchange units during previous expiration, an inspired gas with no inert gas refreshes the gas-exchange units in a later stage of inspiration (350 mL). These considerations suggest that the averaged inert-gas concentration at the entrance of functional gas-exchange unit during inspiration is almost zero under a condition where the MIGET is applied.

(3) The pulsatile nature of blood is disregarded so that capillary blood flow is taken to be continuous. Bidani *et al*[60] analyzed the effect of pulsatile flow (Q_C) and pulsatile capillary blood volume (V_C) on equilibration of O_2 between capillary blood and alveolar gas. They found little difference in O_2 equilibration profile between the condition where both Q_C and V_C are constant and the condition where both Q_C and V_C have pulsatile natures. Therefore, the assumption of constant blood flow may derive no discernable distortion regarding the steady-state gas exchange[61].

(4) The functional gas-exchange unit is assumed to receive capillary blood flow with the same hematocrit. As first suggested by Brisco[62], the gas solubility in erythrocytes is different from that in plasma, indicating that variation in hematocrit between capillaries may affect inert-gas exchange to some extent. However, Young and Wagner[63] demonstrated that although the inert-gas solubility is influenced appreciably by misdistribution of hematocrit, its effect on inert-gas exchange is small.

(5) The inert-gas solubility is taken to be constant irrespective of oxygen saturation with hemoglobin (Hb) (SO_2) and blood pH. Yamaguchi *et al*[64] experimentally demonstrated that SO_2 has no impact, while blood pH has a substantial impact, on the inert-gas solubility, including ethane and cyclopropane, both of which are confined to the protein fraction of blood. However, in the same paper, Yamaguchi *et al*[64] demonstrated that the effect of pH-dependent change in blood solubility of either ethane or cyclopropane on recovered V_A/Q distribution is small.

(6) Diffusion equilibration is assumed to be complete. This assumption applies both to the diffusion between capillary blood and gas phase through alveolocapillary membrane (aqueous-phase diffusion) and to the diffusion within gas phase [gas-phase diffusion (stratification)]. The blood-gas equilibration is valid for any inert gas that does not combine with Hb[52]. However, this assumption is invalid while analyzing the gas combining with Hb, especially carbon monoxide (CO) and nitric oxide (NO)[65].

As argued in the previous section, the stratification is evident in inspiration but not in expiration (Figure 4). Since the MIGET analyzes the gas only collected during expiration, the assumption that the stratification has little impact on gas transfer may be approved in the MIGET condition. Furthermore, Yamaguchi *et al*[66] demonstrated that excepting severe acute respiratory distress syndrome, the stratification plays no role during inert-gas elimination under the condition similar to that of the MIGET. The detailed discussions expanded above identified that most of the physiological assumptions introduced by the MIGET have correct grounds.

Determination of continuous distribution of V_A/Q: Saline containing a small quantity of six foreign inert gases with a wide variety of λ, including sulfur hexafluoride (SF_6) (λ = 0.009 mL/mL at 37 °C), ethane (λ = 0.09), cyclopropane (λ = 0.58), halothane (λ = 2.82), diethyl ether (λ = 14.4), and acetone (λ = 304) was infused through the peripheral vein at a constant rate of 2 mL/min[54,56]. After steady state was established (about 30 min after initiating infusion), expired gas, arterial blood, and

mixed venous blood were simultaneously sampled and the concentrations of six inert gases in the samples were measured by gas chromatography equipped with flame ionization for hydrocarbons and electron capture for SF_6[67]. Using the data measured for six inert gases, Wagner and colleagues[56,58,59] established a novel method allowing for predicting a continuous distribution of V_A/Q in a representative manner. In this method, they assumed the 50 functional gas-exchange units with a variety of V_A/Q values, including the right-to-left shunt with V_A/Q of zero (the number of functional gas-exchange unit: 1), the dead space with infinite V_A/Q (the number: 50) composed of series (common) and parallel (alveolar) dead space, and the 48 units with finite values of V_A/Q ranging from 0.005 to 100, all of which are arranged in parallel and are equally spaced on a logarithmic scale. Applying the least-squares minimization coupled with enforced smoothing under non-negativity constraints for V_A and Q, they determined the distribution of V_A and/or Q along the logarithmic V_A/Q axis. However, it should be noted that the lung model adopted by Wagner *et al*[56,58,59] consists of unknown variables whose number (n = 50) greatly exceeds the number of measured variables (n = 6) so that no unique solution is generally obtainable[68,69]. In principle, the greater the number of gases, the more detailed and precise is the resultant estimate of the V_A/Q distribution. To solve the problem of a non-unique solution, Evans and Wagner[69-73] introduced the linear programing approach, in which the upper limit of V_A and/or Q distributed to a certain V_A/Q unit was examined based on the error of each inert-gas measurement. The linear programming can reliably decide the issue of whether the V_A/Q distribution is unimodal or contains more than one mode, *i.e.*, bimodal or trimodal. The mode of V_A/Q distribution representatively determined by the least-squares minimization was shown to be qualitatively coincident with that by the linear programming[70] (Figure 5). Furthermore, Wagner and West[59,74-76] analyzed the matching between the measured arterial P_{O2} (P_{aO2}) and that predicted from the representative V_A/Q distribution. They found a satisfactory agreement between the two values in patients with chronic obstructive pulmonary disease (COPD) and interstitial pneumonias at rest (Figure 6). However, Wagner[76] found that the P_{aO2} predicted from the MIGET is appreciably higher than the measured P_{aO2} in patients with interstitial pneumonias under an excise condition. This indicates that in addition to the V_A/Q heterogeneity, the aqueous-phase diffusion limitation through alveolocapillary membrane plays some role in worsening hypoxemia during exercise in patients with interstitial pneumonias.

The representative distributions of V_A/Q in normal subjects as well as patients with interstitial pneumonia and COPD are depicted in Figure 7[59]. A normal subject revealed the unimodal distribution of V_A and Q along the V_A/Q axis, which resembles the sharp normal distribution. A patient with interstitial pneumonia showed the bimodal V_A/Q distribution with low V_A/Q regions associated with augmented right-to-left shunt. The formation of low V_A/Q regions and shunt may be ascribed to the interstitial fibrosis-elicited destruction of acinar structures. A COPD patient with predominant emphysema showed the bimodal V_A/Q heterogeneity with high V_A/Q regions, which may be attributed to the regional hyperventilation caused by the destruction of alveoli. A patient with predominant bronchiolar involvements revealed the bimodal V_A/Q heterogeneity with low V_A/Q regions, which may be caused by the destruction and/or obliteration of acinar bronchioles.

Based on the V_A/Q-D/Q concept developed by Piiper[77], in which D denotes the aqueous-phase diffusing capacity for O_2, CO_2, or CO through alveolocapillary membrane, Yamaguchi *et al*[66,78-80] elaborated a novel method that allows for predicting the continuous distribution of V_A/Q and D/Q under a steady-state condition. They[66,78-80] found that in addition to the V_A/Q heterogeneity, the D/Q heterogeneity is expanded in patients with interstitial lung diseases but less evident in patients with COPD (Figure 8). Therefore, it was conceived that the heterogeneity of aqueous-phase diffusion plays some role in impeding gas exchange, particularly in lungs with destruction of alveolocapillary membrane or pulmonary microcirculation.

$AaDO_2$ in classical gas-exchange theory

Determination of alveolar gas composition: About 100 years ago, Krogh *et al*[81] first described the important principle in the field of respiratory physiology; namely, the gas exchange taking place in any lung region is determined by neither the ventilation nor the blood flow but by the ratio of one another. Shortly after this, Haldane[82] recognized that ventilation-perfusion heterogeneity could cause hypoxemia. These pioneering works led Fenn *et al*[83], Riley and Cournand[84], and others into the establishment of classical gas-exchange theory in a more precise fashion. Rahn[85] proposed the concept of "mean alveolar gas" while Riley *et al*[84,86] proposed the concept of "ideal alveolar gas". These two terms are physiologically identical and defined as the intersection of blood and gas R lines, in which R is the respiratory gas-exchange ratio given by the ratio of CO_2 production (V_{CO2}) to O_2 consumption (V_{O2}) of

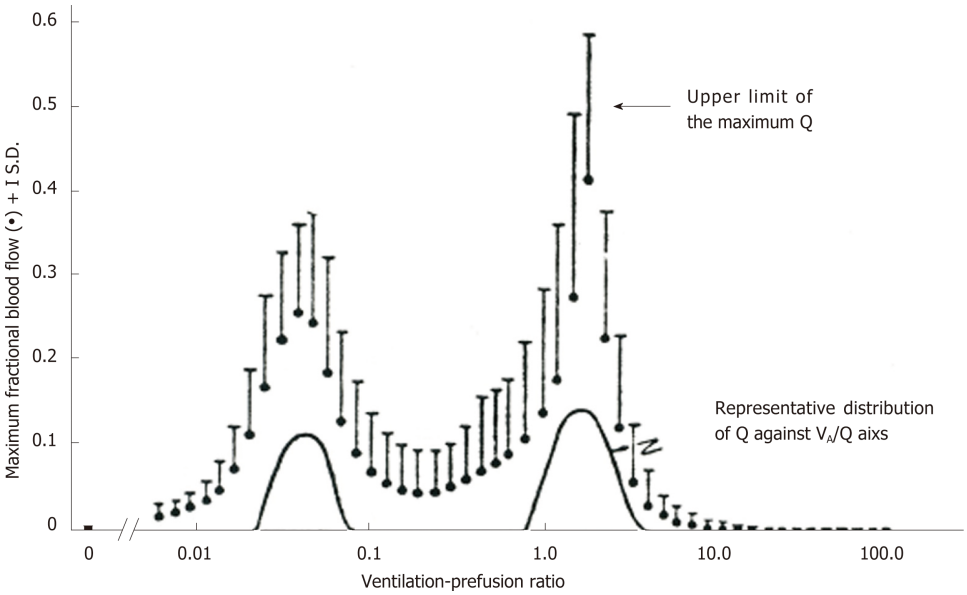

Figure 5 Range of solution for ventilation-perfusion distribution recovered from multiple inert-gas elimination technique. Comparison between representative perfusion distribution obtained from multiple inert-gas elimination technique in terms of least-squares minimization and maximum perfusion distribution decided by linear programming. Adopted from ref[70].

the whole body (Figure 9). As the R is identical at any portion of the body under a steady-state condition, the R values at the level of capillary blood (blood R line) and alveolar gas (gas R line) are the same as that of mixed expired gas. It was theoretically identified that the intersection of the blood R line and gas R line defined the single V_A/Q value and the corresponding unique pair of P_{O2} and P_{CO2} in alveolar gas and capillary blood of a certain lung (the O_2-CO_2 diagram or the V_A/Q line[61,87])[84-86]. Although the P_{O2} and P_{CO2} values thus determined satisfactorily meet the metabolic state of the whole body, it does not secure that these P_{O2} and P_{CO2} can work as the representative indicator while analyzing the gas-exchange behavior in the lung. This is because the concept of mean (ideal) alveolar P_{O2} and P_{CO2} is largely lacking in the considerations on complicatedly intertwined lung anatomy and intricate physiological gas-transfer mechanism along the airways and in the lung periphery. Furthermore, to calculate the mean (ideal) alveolar gas, it is necessary to measure P_{O2} and P_{CO2} in mixed venous blood. As this procedure is cumbersome in a clinical setting, Riley *et al*[86] proposed a new concept of "effective alveolar gas," in which the mean (ideal) alveolar P_{CO2} is taken to equal the arterial P_{CO2} (P_{aCO2}). Because of the relative flatness of blood CO_2 dissociation curve under a physiological condition, the difference between mean (ideal) P_{CO2} and P_{aCO2} is remarkably small (Figure 9), which indicates that it is not unreasonable to use P_{aCO2} in place of mean (ideal) alveolar P_{CO2}. Therefore, P_{aCO2} is defined as "effective alveolar P_{CO2}" and alveolar P_{O2} estimated therefrom is called "effective alveolar P_{O2}". As it is not necessary to measure the gas pressures in mixed venous blood, the concept of effective alveolar P_{O2} has received a great deal of support from physicians, though the anatomical and/or physiological validations on effective alveolar P_{O2} have been lacking. Based on the simplified form of alveolar gas equation, the effective alveolar P_{O2} (effective P_{AO2}) is calculated as

Effective $P_{AO2} = P_{IO2} - P_{aCO2}/R$ ····· eq. 2

Where P_{IO2}, P_{aCO2}, and R denote inspiratory P_{O2}, arterial P_{CO2}, and respiratory gas-exchange ratio, respectively. The R value is taken to be 0.83 in general.

Using eq. 2, one can easily predict the effective alveolar-arterial P_{O2} difference (effective $AaDO_2$) at the bed side as:

Effective $AaDO_2$ = effective P_{AO2} – measured P_{aO2} ····· eq. 3

Unless otherwise specified, P_{AO2} and $AaDO_2$ indicate effective P_{AO2} and effective $AaDO_2$, respectively in this review.

Relationships between $AaDO_2$ and V_A/Q distribution decided by MIGET: Differing from the V_A/Q theory developed on the basis of the MIGET, the classical gas-exchange theory is not sufficiently warranted by the anatomical and physiological facts. Hence, it is necessary for certifying the issue of whether the effective P_{AO2} indeed functions as the representative P_{O2} in mixed gas exhaled from all functional gas-exchange units. For answering this question, it is indispensable at least to compare the results obtained from the classical gas-exchange theory with those from the MIGET.

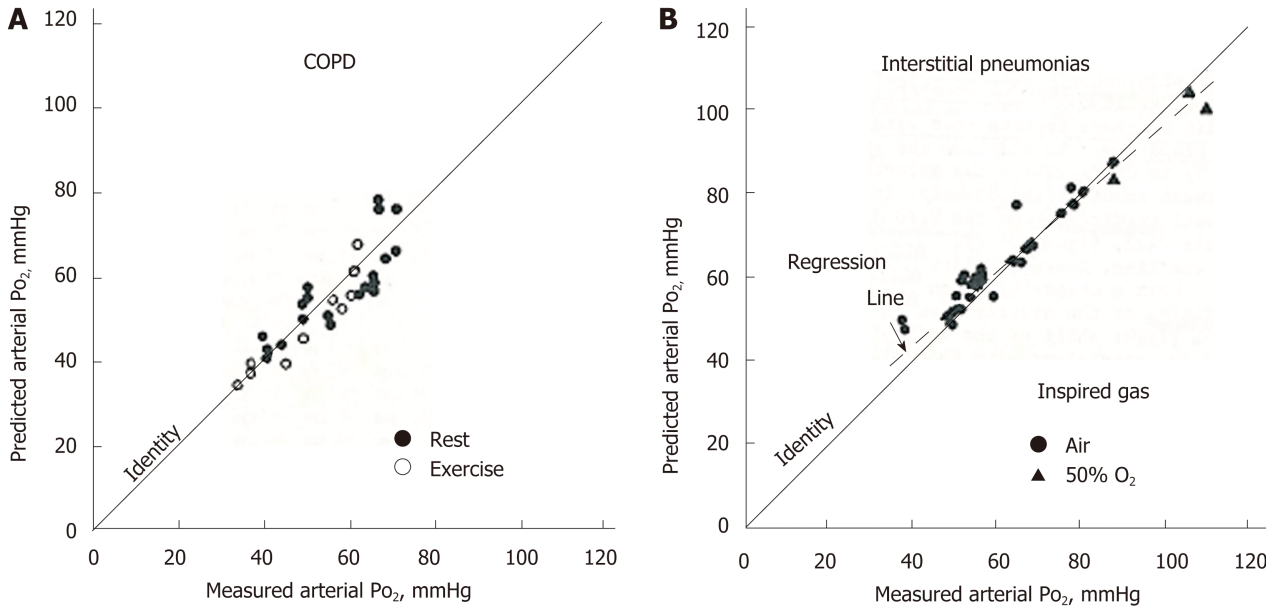

Figure 6 Comparison of predicted P_{aO2} from multiple inert-gas elimination technique and measured P_{aO2}. A: Chronic obstructive pulmonary disease at rest or during exercise; B: Interstitial pneumonias at rest while inspiring gas with 21% O_2 (room air) or 50% O_2. Adopted from ref[76]. COPD: Chronic obstructive pulmonary disease.

We first examined what kinds of V_A/Q units are sensitively detected by O_2. We calculated P_{AO2} in each V_A/Q unit on the assumption that P_{O2} equilibration between alveolar gas and capillary blood is complete (Figure 10). We found that P_{AO2} changes sharply in the units having V_A/Q ranging from 0.1 to 1.0, (*i.e.*, the sensitivity of O_2 to V_A/Q detection is equivalent to that of cyclopropane) but not in other V_A/Q units, suggesting that $AaDO_2$ reflects gas-exchange behavior in regions with moderately low V_A/Q values but is insensitive to gas exchange in regions with very low and high V_A/Q values. The finding indicated that the ability of $AaDO_2$ detecting the V_A/Q heterogeneity was substantially limited and does not cover the whole range of V_A/Q heterogeneity as the MIGET does.

Next, we investigated the coincidence between mixed P_{AO2} estimated from V_A/Q distribution recovered from the MIGET and effective P_{AO2} calculated from eq. 2 in patients with interstitial pneumonia or COPD (Figure 11). The coincidence between the two P_{AO2} was satisfactory, indicating that the effective P_{AO2} and effective $AaDO_2$ can accordingly change reflecting the formation of moderately low V_A/Q regions that is related to the emergence of hypoxemia. Hence, we concluded that effective P_{AO2} and effective $AaDO_2$ are practically useful in a clinical setting as far as the gas-exchange abnormality elicited by moderately low V_A/Q regions is considered.

Pulmonary diffusing capacity for CO (D_{LCO})

General survey on D_{LCO}: The most terminal organization in the lung is alveolocapillary membrane and capillary network embedded in the alveolar wall (septum) (Figure 12). The main mechanism of gas transfer through alveolocapillary membrane and capillary blood is the aqueous-phase diffusion so that the impaired gas transfer there is estimated by measuring the pulmonary diffusing capacity using diffusion-limited gases such as CO and NO, *i.e.*, D_{LCO} and D_{LNO} (Figure 13). About 30 years ago, Guénard *et al*[88] and Borland and Higginbottom[89] independently elaborated a method for measuring the D_{LNO}. NO has an extremely high affinity with Hb, *i.e.*, 400000 times higher than that of O_2 and 1800 times higher than that of CO[65], which indicates that the chemical reaction of NO with Hb has virtually no obstacle to NO uptake by erythrocytes (*i.e.*, diffusion limitation but no reaction limitation). Therefore, the partial pressure of NO in pulmonary capillary network is assumed to be practically zero, suggesting that D_{LNO} may be predominantly decided by the diffusive process across alveolocapillary membrane and erythrocytes. However, this does not hold true in the case of D_{LCO}, in which besides the diffusive process across alveolocapillary membrane and erythrocytes, the replacement reaction of CO with HbO_2 causes a substantial resistance to CO transfer, *i.e.*, diffusion limitation plus reaction limitation. In the current review, we will confine ourselves to describe D_{LCO} only. This is simply because D_{LNO} is not presently measured worldwide. If readers want to know a more comprehensive discussion on D_{LCO} and D_{LNO}, we refer them to a

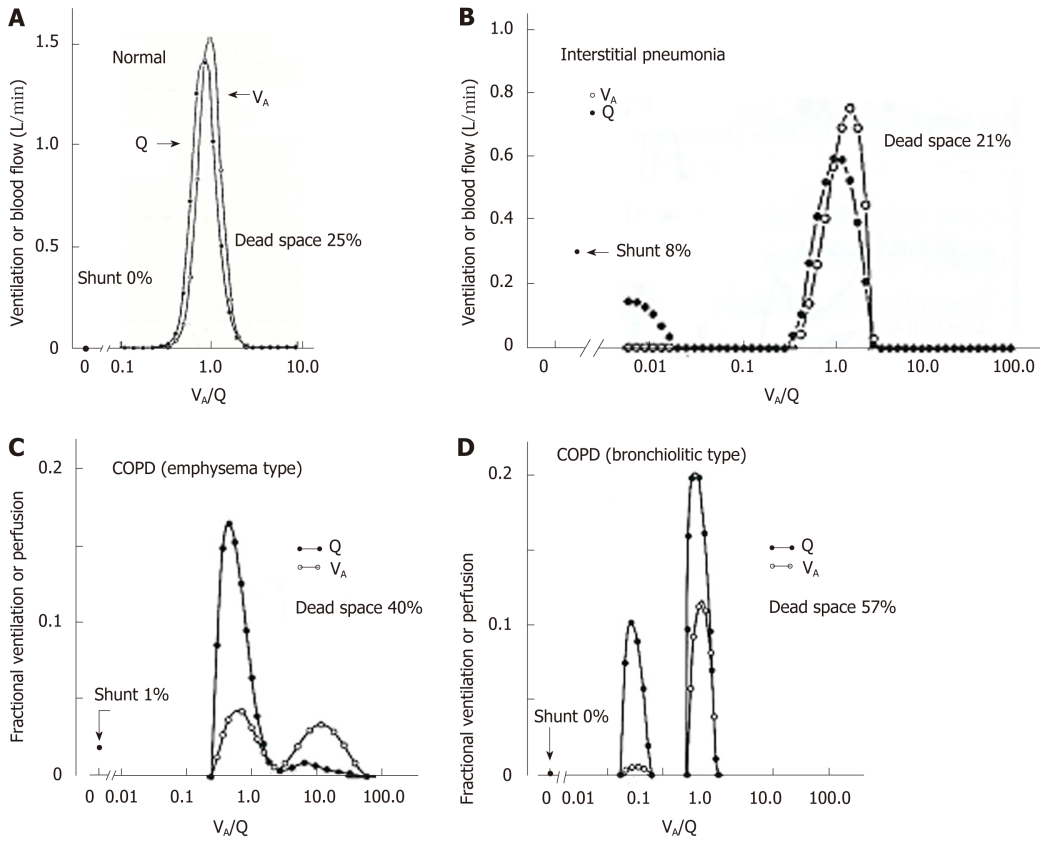

Figure 7 Representative ventilation-perfusion distributions predicted from multiple inert-gas elimination technique in various types of lung diseases. A: Young normal subject; B: Patient with interstitial pneumonia; C: Chronic obstructive pulmonary disease patient with predominant emphysema; D: Chronic obstructive pulmonary disease patient with predominant bronchiolitis. See text for detailed explanation. Adopted from ref[59]. V_A/Q: Ventilation-perfusion; COPD: Chronic obstructive pulmonary disease.

more extensive review reported by us[65].

It has been over 100 years since Krogh[90] developed the method to measure the single-breath CO uptake through alveolocapillary membrane. Since then, the single-breath D_{LCO} has gained a position as the most clinically useful pulmonary function test after spirometry and lung volume examination. The practical method to examine the single-breath D_{LCO} was proposed by Ogilvie *et al*[91]. Concurrently, Roughton *et al*[92] proposed an important model describing the gas transfer through alveolocapillary membrane and erythrocytes. They assumed that the CO transfer process from alveolocapillary membrane to Hb condensed within erythrocytes could be simplified into the two processes; *i.e.*, (1) the membrane diffusing capacity for CO (D_{MCO}) that reflects the diffusion limitation across alveolocapillary membrane and plasma layer surrounding erythrocytes, and (2) the blood diffusing capacity for CO (D_{BCO}) that is defined as the product of capillary blood volume (V_C) and specific gas conductance for CO in the blood (θ_{CO}). The θ_{CO} signifies the diffusive process across erythrocyte membrane and its interior incorporated with the competitive replacement reaction of CO with HbO_2. Since the reciprocals of D_{MCO} and D_{BCO} are the gas-transfer resistances that are connected in series, the total resistance for CO transfer, $1/D_{LCO}$, is expressed as

$$1/D_{LCO} = 1/D_{MCO} + 1/(\theta_{CO} \cdot V_C) \cdots\cdots \text{eq. 4}$$

In addition to the D_{LCO}, the D_{LCO}/V_{AV}, in which V_{AV} denotes the alveolar volume during a single-breath maneuver, is similarly important. This parameter expresses the D_{LCO} per unit alveolar volume, which is equal to the Krogh factor (K_{CO}), *i.e.*, the rate constant of alveolar gas uptake per unit pressure. The relative contribution of $1/D_{MCO}$ and that of $1/D_{BCO}$ to overall resistance of CO transfer ($1/D_{LCO}$) were found to be 23% and 77%, respectively (Figure 14)[65,93]. The finding indicated that D_{LCO} is primarily weighted by D_{BCO}, suggesting that D_{LCO}-associated parameters are more susceptible to the damage of pulmonary microcirculation than that of alveolocapillary membrane.

Factors affecting D_{LCO} and K_{CO}: The D_{LCO} and K_{CO} are the physiological parameters that are useful for diagnosing the pathological changes occurring in alveolocapillary membrane and pulmonary microcirculation. However, there are many matters that

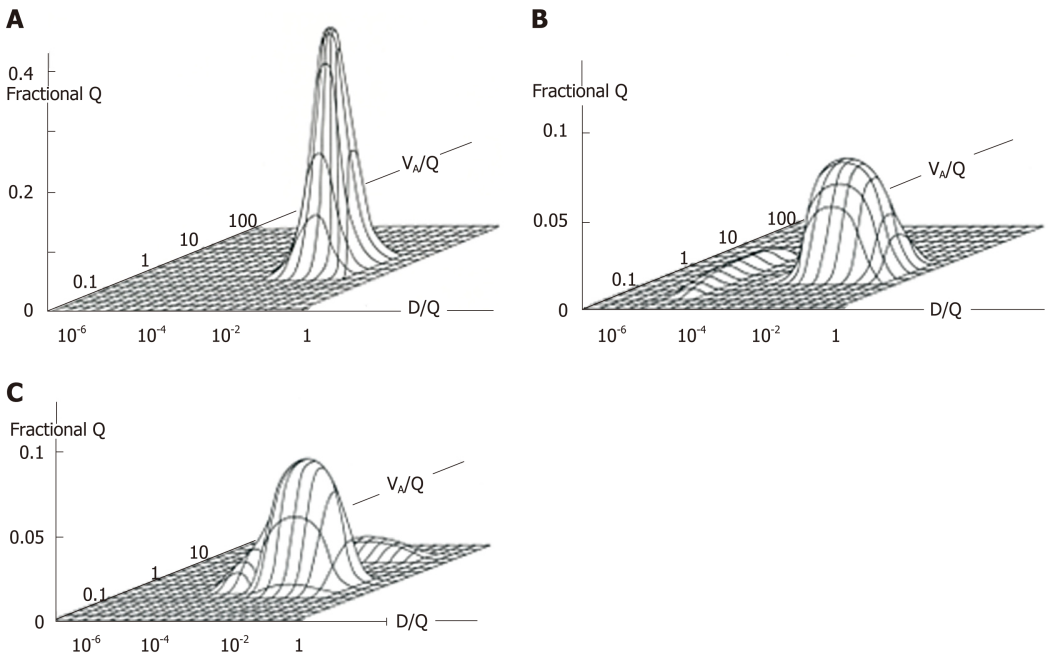

Figure 8 Ventilation-perfusion (V_A/Q)-Diffusing capacity-perfusion (D/Q) distributions in normal and diseased lungs. A: V_A/Q and D/Q distribution in normal lung; B: That in lung with desquamative interstitial pneumonia; C: That in lung with chronic obstructive pulmonary disease characterized by emphysema. Patient with desquamative interstitial pneumonia (B) revealed minimal V_A/Q heterogeneity but very low D/Q regions that may yield "diffusion shunt" contributing to hypoxemia. Very low D/Q regions may be caused by decreased surface area and/or increased thickness of alveolocapillary membrane. Patient with chronic obstructive pulmonary disease (C) showed V_A/Q heterogeneity with high V_A/Q regions but minimal regions with very low D/Q. Modified from ref[80].

should be argued with regard to the D_{LCO}-related parameters as listed below.

Influence of back-pressure of CO from pulmonary capillary blood: The CO back-pressure during D_{LCO} measurement is estimated at about 3% of the alveolar P_{CO} in a nonsmoking subject[65]. Therefore, the effect of CO back-pressure on D_{LCO} can be ignored in a subject with no habitual smoking. However, heavy smokers or repeated measurements of D_{LCO} produced the CO back-pressure that is not disregarded because the CO back-pressure reaches about 16% of the alveolar P_{CO}, which induces a significant error while estimating the overall D_{LCO}.

Influence of functional heterogeneities: The D_{LCO} is influenced by at least three heterogeneities[65]; (1) the distribution of alveolar tidal volume to alveolar volume (V_{AT}/V_{AV}), (2) that of diffusing capacity to alveolar volume (D_{LCO}/V_{AV}, *i.e.*, K_{CO}), and (3) that of alveolar tidal volume in each region to total alveolar tidal volume. Of these, the heterogeneity of K_{CO}, which may be caused by the regional difference in rate constant of CO uptake due to local variations in the thickness of alveolocapillary membrane and plasma layer as well as the density of erythrocytes in microcirculation[94], is the most important, while other two heterogeneities may be considerably degraded during a breath-holding maneuver. Piiper and Sikand[95,96] theoretically and experimentally analyzed the significance of K_{CO} heterogeneity on overall D_{LCO}, resulting in a larger D_{LCO} value for a shorter breath-hold time. Furthermore, their analysis[95,96] identified that the overall D_{LCO} may be underestimated by 37% in a condition where a serious K_{CO} heterogeneity exists. However, it is impossible to universally apply the value reported by Piiper and Sikand[95,96] to clinical cases having various types of lung diseases because the extent of K_{CO} heterogeneity differs substantially in respective patients. Therefore, the measured D_{LCO} should be regarded as the "apparent or effective" value that is always underestimated by the K_{CO} heterogeneity to an uncertain extent.

To note, if the diffusing capacity (D) for a certain gas is measured under a steady-state condition, the apparent D value is significantly reduced due to the V_A/Q and D/Q heterogeneities. Indeed, Yamaguchi *et al*[80] identified an appreciable effect of these heterogeneities on apparent D value, particularly in patients with interstitial lung diseases (Figure 8).

Influence of alveolar volume: Declining alveolar volume (V_{AV}) without loss of acini (for instance, inspiratory muscle insufficiency) accompanies[65,97]: (1) slight decrease in D_{MCO}/V_{AV} but large increase in V_C/V_{AV}, (2) decrease in D_{LCO}, and (3) increase in K_{CO}, which indicates the "facilitated" CO transfer per unit lung volume in conditions with declining V_{AV} with no loss of acini. Overall V_C remains constant due to the stability of

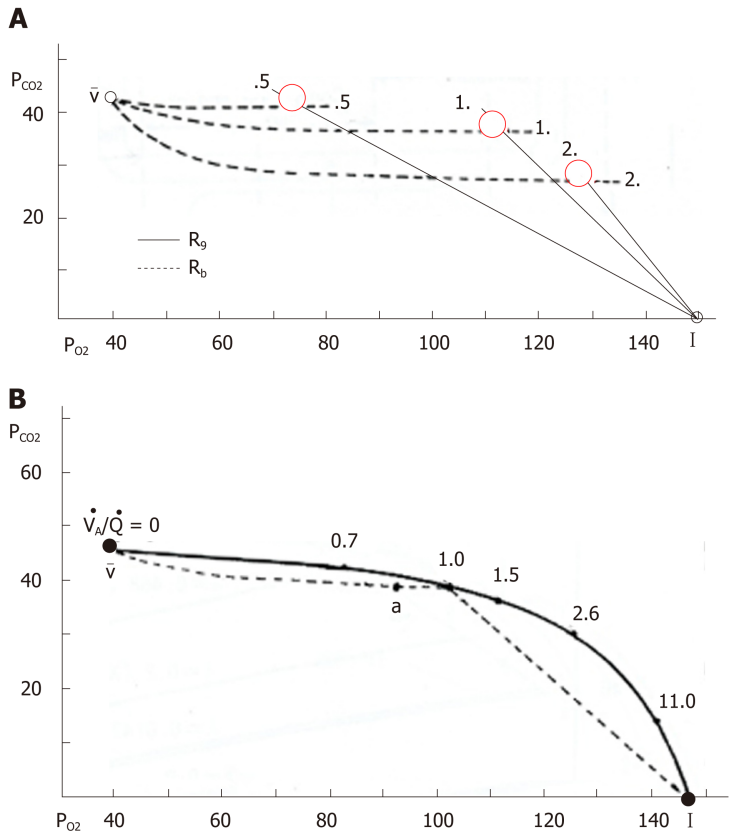

Figure 9 O_2-CO_2 diagram and ventilation-perfusion line. A: O_2-CO_2 diagram, in which solid and dotted lines indicate gas R lines and blood R lines, respectively. Intersection of these two lines denoted by red circle provides a single ventilation-perfusion value and corresponding unique pair of P_{O2} and P_{CO2}; B: Ventilation-perfusion line constructed by connecting each intersection of gas R lines and blood R lines. I: Inspired point; a: Arterial point; v: Mixed venous point. See text for further explanation. Adopted from ref[87].

cardiac output (Q), which reinforces the redistribution of pulmonary perfusion during lung volume changes; thus V_C/V_{AV} increases with decreasing V_{AV}. Reduced V_{AV} decreases D_{MCO} but does not change V_C, leading to decreased D_{LCO}. Hence, the characteristic of decreased V_{AV} without loss of acini is decreased D_{LCO} in association with increased K_{CO}.

The situation is different in the diminished expansion caused by loss of acini such as post-pnemonectomy. Declining V_{AV} with losing acini elicits[65,97]: (1) decrease in both D_M and V_C associated with large decrease in D_{LCO}, (2) small increase in V_C/V_{AV} accompanied with increased D_{MCO}/V_{AV} (this is attributed to the redistribution of Q), and (3) small change in K_{CO}. The trend of D_{MCO}/V_{AV} is opposite to that without loss of acini. The extent of increased V_C/V_{AV} in lungs with loss of acini is less than that without loss of acini, leading to a restricted increase in K_{CO} (*i.e.*, a lesser improvement of CO uptake per unit lung volume) in lungs with losing acini.

Influence of cardiac output: The increased Q (for instance, left-to-right shunt) elicits capillary distension and/or recruitment, leading to the increased surface area of alveolocapillary membrane (rise in D_{MCO} and D_{MCO}/V_{AV}) and the augmented capillary blood volume (rise in V_C and V_C/V_{AV}), which increase both D_{LCO} and K_{CO}. On the other hand, decreased Q shows the opposite trend[98,99].

Influence of alveolar hemorrhage: The behaviors of D_{LCO} and K_{CO} in patients with alveolar hemorrhage (for instance, ANCA-associated microscopic polyangiitis) are qualitatively similar to those observed in patients with increased Q. This is because hemorrhage-derived Hb released into the alveolar space absorbs CO before it reaches the capillary blood such that both D_{LCO} and K_{CO} are elevated even under a condition where alveolar walls are significantly injured.

Differential diagnosis based on behaviors of D_{LCO} and K_{CO}: The decrease in both D_{LCO} and K_{CO} is the general feature in lungs with various injuries of alveolocapillary membrane and/or pulmonary microcirculation because they reduce D_{MCO}, D_{BCO}, or both. We want to define these general behaviors of D_{LCO} and K_{CO} as the type-1 abnormality. However, there are many pathological conditions that do not follow the

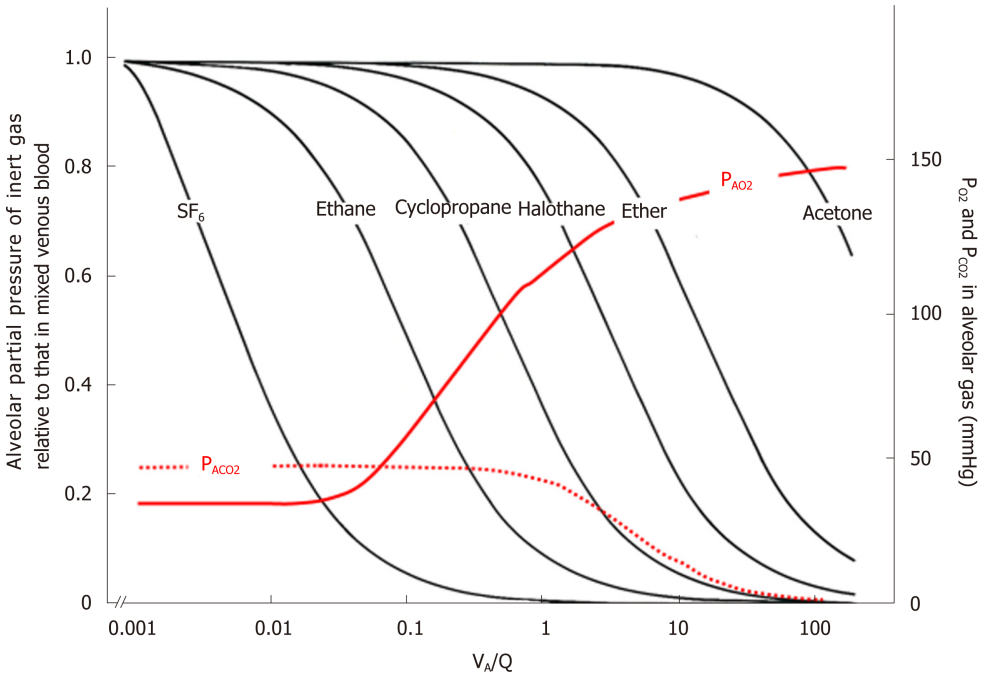

Figure 10 Ventilation-perfusion (V_A/Q) regions detected from gas exchange behaviors of O_2, CO_2, and inert gases. Left ordinate: excretion (E) of inert gas defined as P_A/P_v, where P_A is partial pressure of inert gas in each functional gas-exchange unit, while P_v is that in mixed venous blood. Right ordinate: P_{AO2} and P_{ACO2} in each functional gas-exchange unit. Abscissa: logarithmic V_A/Q value. E of each inert gas sharply changes in a certain range of V_A/Q depending on its blood-gas partition coefficient (λ). For instance, sharp change in E for SF_6 is found at V_A/Q ranging between 0.001 and 0.01. As such, SF_6 has high sensitivity to detecting gas exchange in regions with very low V_A/Q. On the other hand, E for acetone sharply changes at V_A/Q ranging from 10 to 100, indicating that acetone is susceptible to gas exchange in regions with very high V_A/Q. P_{AO2} changes greatly at V_A/Q ranging between 0.1 and 1.0, suggesting that O_2 has sensitivity to detecting gas exchange in regions with moderately low V_A/Q (like cyclopropane). Meanwhile, CO_2 is susceptible to gas exchange in regions with moderately high V_A/Q ranging from 1.0 to 10 (like halothane).

principle of type-1 abnormality. As discussed above, declining alveolar volume without loss of acini leads to decreased D_{LCO} in association with increased K_{CO}. We define these behaviors of D_{LCO} and K_{CO} as the type-2 abnormality. On the other hand, declining alveolar volume with losing acini elicits decreased D_{LCO} and restricted rise in K_{CO}. We define these aspects of D_{LCO} and K_{CO} as the type-3 abnormality. Increased Q and alveolar hemorrhage increase both D_{LCO} and K_{CO}. We define these increasing aspects of D_{LCO} and K_{CO} as the type-4 abnormality.

In 1951, Austrian *et al*[100] first proposed the disease concept of "alveolar-capillary (A-C) block." This classic syndrome originated to describe the interference of gas transfer through alveolocapillary membrane by aqueous-phase diffusion in patients with various kinds of interstitial lung disease[101,102]. However, many physiologists and clinicians have questioned the role of impaired aqueous-phase diffusion as the factor inducing hypoxemia. This is because in addition to alveolar interstitium, acinar airways and pulmonary microcirculation are simultaneously injured in most of the interstitial lung diseases. The impediment of acinar airways and/or microcirculation evokes the V_A/Q heterogeneity leading to hypoxemia. In relation to this problem, there has been no direct study credibly addressing the issue of whether the impaired aqueous-phase diffusion across alveolocapillary membrane can indeed evoke hypoxemia. To answer this question, all gas-exchange parameters, including V_A/Q distribution, $AaDO_2$, D_{LCO}, and K_{CO}, should be simultaneously examined in patients with pathologically-confirmed pure lesion of impaired alveolocapillary membrane but no lesion of acinar airways or pulmonary microcirculation.

CONCLUSION

To answer the questions that have remained unsolved in the field of respiratory physiology, we analyzed the structure-function relationships in the lung from a variety of anatomical and physiological points of view. The important results found therefrom are as follows: (1) The model A of Weibel is useful for estimating gas mixing in peripheral conducting airways; (2) The anatomical gas-exchange unit is organized by the acinus of Loeschcke; (3) Although it is difficult to define the functional gas-exchange unit correctly, the acinus of Aschoff may act as the functional

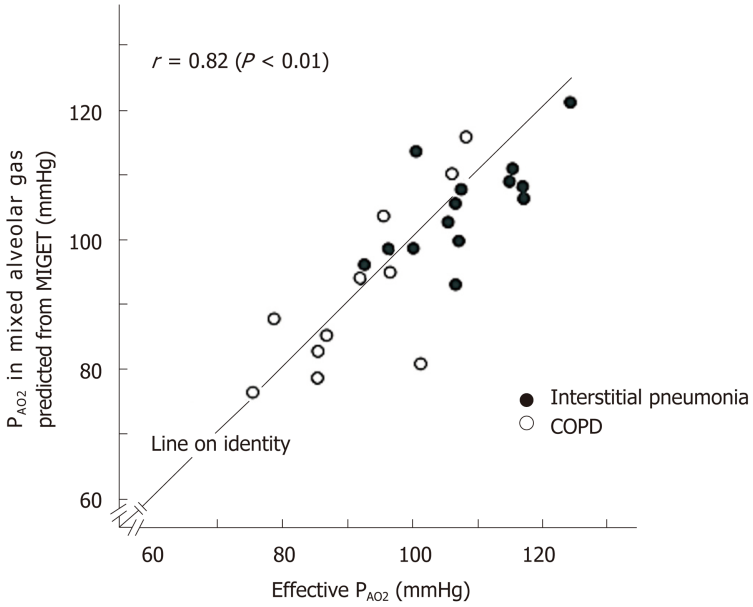

Figure 11 Comparison of effective P_{AO2} and P_{AO2} in mixed alveolar gas estimated from ventilation-perfusion distribution decided by multiple inert-gas elimination technique. Effective P_{AO2} and P_{AO2} estimated from multiple inert-gas elimination technique were compared [patients with interstitial pneumonia (*n* = 14) and chronic obstructive pulmonary disease (*n* = 11)]. Coincidence of two P_{AO2} is satisfactory. See text for further explanation.

gas-exchange unit in an initial approximation; (4) The MIGET is supported by the anatomical and physiological backgrounds in many respects. Therefore, the MIGET is clinically valuable for predicting the heterogeneous V_A/Q distribution between the acini of Aschoff under steady-state conditions; (5) The effective $AaDO_2$ sensitively detects moderately low V_A/Q regions causing hypoxemia. Hence, the $AaDO_2$ is taken as a useful, clinical indicator for predicting impaired gas exchange. However, one should be aware that the $AaDO_2$ is insensitive to impaired gas exchange caused by very low V_A/Q regions and/or high V_A/Q regions; (6) The D_{LCO} and K_{CO} (D_{LCO}/V_{AV}) are useful for diagnosing the impediment of alveolar walls, including alveolocapillary membrane and pulmonary microcirculation. However, one should recognize the fact that the effect of regional variations in K_{CO} on overall D_{LCO} could not be totally eliminated; and (7) The clinically useful categorization with regard to behaviors of D_{LCO} and K_{CO} is the type-1 abnormality (decrease in both D_{LCO} and K_{CO}), the type-2 abnormality (decrease in D_{LCO} but increase in K_{CO}), the type-3 abnormality (decrease in D_{LCO} but restricted rise in K_{CO}), or the type-4 abnormality (increase in both D_{LCO} and K_{CO}). These categories of D_{LCO} and K_{CO} abnormalities allow for precise differential diagnosis concerning the damage in alveolocapillary membrane and that in pulmonary microcirculation.

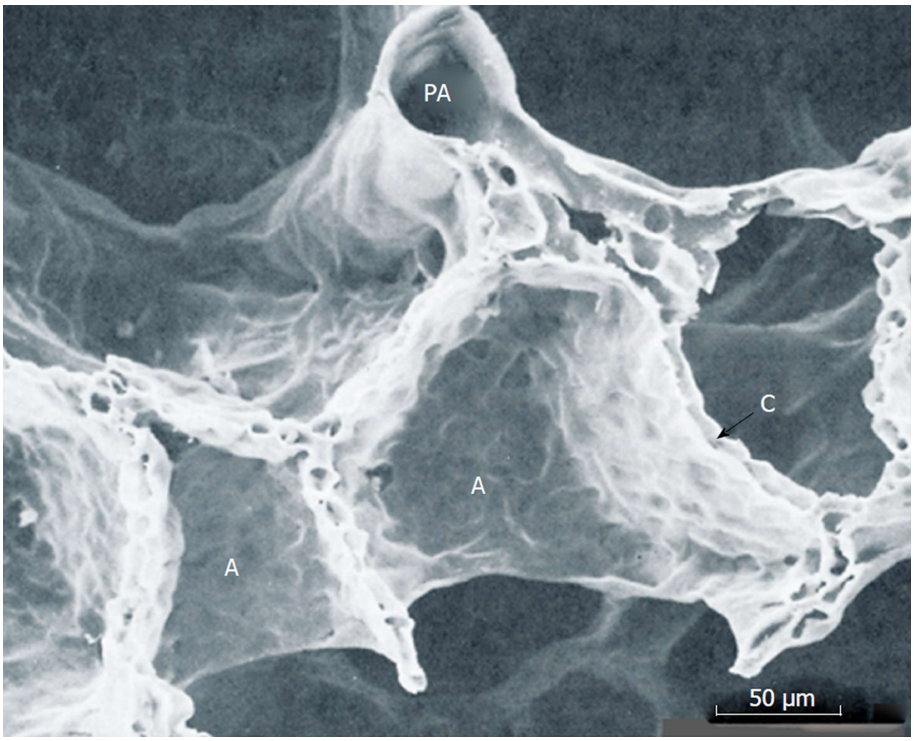

Figure 12 Scanning electron microscopic image of perfusion-fixed alveolar walls. PA: Pulmonary arteriole; A: Alveolar walls, C: Capillary networks embedded in alveolar wall. Adopted from ref[25].

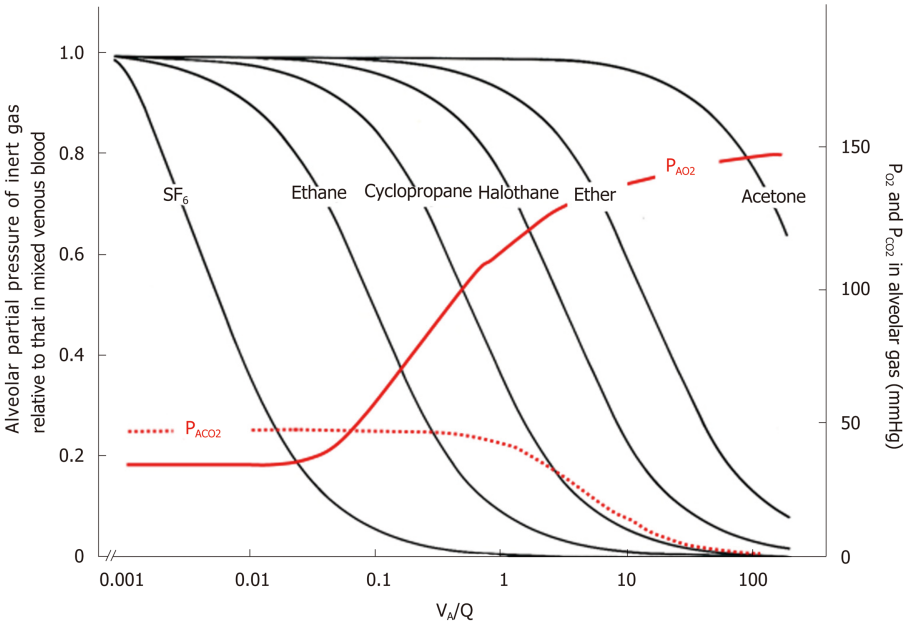

Figure 13 Partial-pressure equilibration of gases between alveolar gas and capillary blood. Inert gases that are not combined with erythrocyte hemoglobin (Hb) show instantaneous equilibration between alveolar gas and capillary blood. O_2 and CO_2 that have relatively low affinity with Hb need some time for completing equilibration between alveolar gas and capillary blood. CO and NO (red lines) that have very high affinity with Hb prevent rise in their partial pressures in capillary blood. Hence, CO and NO do not reach partial-pressure equilibration between alveolar gas and capillary blood any more even in normal lung. Affinity of NO with Hb is extremely high and chemical reaction of NO with Hb is very rapid such that partial pressure of NO in capillary blood is maintained at negligible level. Therefore, there is no "back-pressure" effect during measurement of D_{LNO}. However, affinity of CO with Hb is lower than that of NO (*i.e.*, 1/1800 times that of NO). Therefore, partial pressure of CO in capillary blood rises gradually such that "back-pressure" of CO from capillary blood should not be ignored while measuring the pulmonary diffusing capacity for CO.

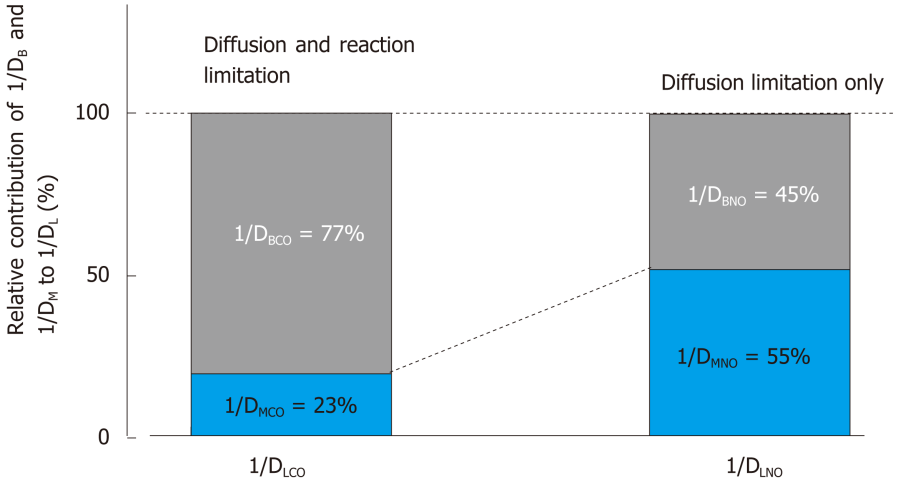

Figure 14 Relative contribution of $1/D_M$ and $1/D_B$ to overall resistance of $1/D_L$. Difference in membrane diffusing capacity for CO (D_{MCO}) and that for NO (D_{MNO}) is simply attributed to difference in their Krogh diffusion constants defined as (α·d), where α is Bunsen solubility coefficient of the gas (mL/mL/atm) and d is gas diffusivity (cm^2/s) in alveolocapillary membrane and plasma layer. D_{MNO}/D_{MCO} is assumed to be 1.97[65]. On the other hand, blood-diffusing capacity for CO (D_{BCO}) or NO (D_{BNO}) is defined as alveolar capillary blood volume (V_C) multiplied by specific gas conductance of each gas (θ_{CO}, θ_{NO}). θ_{CO} signifies the diffusive process across erythrocyte membrane and its interior incorporated with the competitive, replacement reaction of CO with hemoglobin O_2. Therefore, θ_{CO} changes significantly depending on surrounding P_{O2}. On the other hand, θ_{NO} is not influence by chemical reaction with hemoglobin and is predominant by diffusion across erythrocytes, thus resulting in constant θ_{NO} [4.5 mL/min/mmHg/(mL×blood)[65,93]]. The pulmonary diffusing capacity for CO is primarily governed by both diffusion through alveolocapillary membrane and erythrocytes as well as reaction in erythrocytes (limitation by both diffusion and reaction), whereas the pulmonary diffusing capacity for NO is almost evenly prescribed by diffusion through alveolocapillary membrane and that inside erythrocytes (diffusion limitation only). Important message drawn from this analysis is that the pulmonary diffusing capacity for NO is evenly sensitive to morphological abnormality in alveolocapillary membrane as well as that in pulmonary microcirculation. On the other hand, the pulmonary diffusing capacity for CO is more sensitive to microcirculatory abnormality. Adopted from ref[65].

REFERENCES

1 **James DG**, Studdy PR. A Color Atlas of Respiratory Diseases, volume 2. London: Wolfe Medical Publications Ltd 1981; 1-29
2 **Weibel ER**. Design of airways and blood vessels considered as branching trees. The LUNG Scientific Foundations (second edition). Philadelphia: Lippincott-Raven Publishers 1997; 1061-1071
3 **Gehr P**, Bachofen M, Weibel ER. The normal human lung: ultrastructure and morphometric estimation of diffusion capacity. *Respir Physiol* 1978; **32**: 121-140 [PMID: 644146 DOI: 10.1016/0034-5687(78)90104-4]
4 **Phalen RF**, Yeh HC, Schum GM, Raabe OG. Application of an idealized model to morphometry of the mammalian tracheobronchial tree. *Anat Rec* 1978; **190**: 167-176 [PMID: 629400 DOI: 10.1002/ar.1091900202]
5 **Phalen RF**, Oldham MJ, Beaucage CB, Crocker TT, Mortensen JD. Postnatal enlargement of human tracheobronchial airways and implications for particle deposition. *Anat Rec* 1985; **212**: 368-380 [PMID: 4073554 DOI: 10.1002/ar.1092120408]
6 **Horsfield K**, Dart G, Olson DE, Filley GF, Cumming G. Models of the human bronchial tree. *J Appl Physiol* 1971; **31**: 207-217 [PMID: 5558242 DOI: 10.1152/jappl.1971.31.2.207]
7 **Horsfield K**. Axial pathways compared with complete data in morphological studies of the lung. *Respir Physiol* 1984; **55**: 317-324 [PMID: 6739988 DOI: 10.1016/0034-5687(84)90054-9]
8 **Haefeli-Bleuer B**, Weibel ER. Morphometry of the human pulmonary acinus. *Anat Rec* 1988; **220**: 401-414 [PMID: 3382030 DOI: 10.1002/ar.1092200410]
9 **Raskin SP**, Herman PG. Interacinar pathways in the human lung. *Am Rev Respir Dis* 1975; **111**: 489-495 [PMID: 1092234 DOI: 10.1164/arrd.1975.111.4.489]
10 **Webb WR**. Thin-section CT of the secondary pulmonary lobule: anatomy and the image--the 2004 Fleischner lecture. *Radiology* 2006; **239**: 322-338 [PMID: 16543587 DOI: 10.1148/radiol.2392041968]
11 **Weibel ER**. Is the lung built reasonably? The 1983 J. Burns Amberson Lecture. *Am Rev Respir Dis* 1983; **128**: 752-760 [PMID: 6414351 DOI: 10.1164/arrd.1983.128.4.752]
12 **Horsfield K**, Cumming G. Morphology of the bronchial tree in man. *J Appl Physiol* 1968; **24**: 373-383 [PMID: 5640724 DOI: 10.1152/jappl.1968.24.3.373]
13 **Hogg JC**, Hackett TL. Structure and Function Relationships in Diseases of the Small Airways. *Ann Am Thorac Soc* 2018; **15**: S18-S25 [PMID: 29461883 DOI: 10.1513/AnnalsATS.201710-809KV]
14 **Yeh HC**, Schum GM. Models of human lung airways and their application to inhaled particle deposition. *Bull Math Biol* 1980; **42**: 461-480 [PMID: 7378614 DOI: 10.1007/BF02460796]
15 **Itoh H**, Murata K, Konishi J, Nishimura K, Kitaichi M, Izumi T. Diffuse lung disease: pathologic basis for the high-resolution computed tomography findings. *J Thorac Imaging* 1993; **8**: 176-188 [PMID: 8320761]
16 **Webb WR**, Müller NL, Naidich DP. Illustrated glossy of high-resolution computed tomography. In: High-Resolution CT of the Lung (third edition). Philadelphia: Lippincott Williams & Wilkins 2001; 599-618
17 **Reid L**, Simon G. The peripheral pattern in the normal bronchogram and its relation to peripheral pulmonary anatomy. *Thorax* 1958; **13**: 103-109 [PMID: 13569411 DOI: 10.1136/thx.13.2.103]
18 **Reid L**. The secondary lobule in the adult human lung, with special reference to its appearance in bronchograms. *Thorax* 1958; **13**: 110-115 [PMID: 13569412 DOI: 10.1136/thx.13.2.110]

19 **Yamaguchi K**. Morphological and biological alterations determining ventilation-perfusion inequality in the lung. *Kokyu* 1995; **14**: 281-287
20 **Lee JY**, Lee KS, Jung KJ, Han J, Kwon OJ, Kim J, Kim TS. Pulmonary tuberculosis: CT and pathologic correlation. *J Comput Assist Tomogr* 2000; **24**: 691-698 [PMID: 11045687 DOI: 10.1097/00004728-200009000-00005]
21 **Hansen JE**, Ampaya EP, Bryant GH, Navin JJ. Branching pattern of airways and air spaces of a single human terminal bronchiole. *J Appl Physiol* 1975; **38**: 983-989 [PMID: 1141138 DOI: 10.1152/jappl.1975.38.6.983]
22 **Paiva M**, Engel LA. Model analysis of gas distribution within human lung acinus. *J Appl Physiol Respir Environ Exerc Physiol* 1984; **56**: 418-425 [PMID: 6706753 DOI: 10.1152/jappl.1984.56.2.418]
23 **La Force RC**, Lewis BM. Diffusional transport in the human lung. *J Appl Physiol* 1970; **28**: 291-298 [PMID: 5414760 DOI: 10.1152/jappl.1970.28.3.291]
24 **Piiper J**, Scheid P, Fishman AP, LE Farhi, Tenney SM, Geiger SR. In: Fishman AP, LE Farhi, Tenney SM, Geiger SR. Handbook of Physiology, section 3: The Respiratory System, volume IV. Fishman AP, LE Farhi, Tenney SM, Geiger SR. Bethesda Maryland: American Physiological Society 1987; 51-69
25 **Weibel ER**. Design and morphometry of the pulmonary gas exchanger. The LUNG Scientific Foundations (second edition). Philadelphia: Lippincott-Raven Publishers 1997; 1147-1157
26 **Schreider JP**, Hutchens JO. Morphology of the guinea pig respiratory tract. *Anat Rec* 1980; **196**: 313-321 [PMID: 7406223 DOI: 10.1002/ar.1091960307]
27 **Mitzner W**. Collateral ventilation. The LUNG Scientific Foundations (second edition). Philadelphia: Lippincott-Raven Publishers 1997; 1425-1435
28 **Lambert MW**. Accessory bronchiole-alveolar communications. *J Pathol Bacteriol* 1955; **70**: 311-314 [PMID: 13295905 DOI: 10.1002/path.1700700206]
29 **Duguid JB**, Lambert MW. The pathogenesis of coal miner's pneumoconiosis. *J Pathol Bacteriol* 1964; **88**: 389-403 [PMID: 14226413 DOI: 10.1002/path.1700880203]
30 **Martin HB**. Respiratory bronchioles as the pathway for collateral ventilation. *J Appl Physiol* 1966; **21**: 1443-1447 [PMID: 5923213 DOI: 10.1152/jappl.1966.21.5.1443]
31 **Boyden EA**. The structure of the pulmonary acinus in a child of six years and eight months. *Am J Anat* 1971; **132**: 275-299 [PMID: 5115520 DOI: 10.1002/aja.1001320302]
32 **Sobin SS**, Fung YC, Lindal RG, Tremer HM, Clark L. Topology of pulmonary arterioles, capillaries, and venules in the cat. *Microvasc Res* 1980; **19**: 217-233 [PMID: 7382846 DOI: 10.1016/0026-2862(80)90042-4]
33 **König MF**, Lucocq JM, Weibel ER. Demonstration of pulmonary vascular perfusion by electron and light microscopy. *J Appl Physiol***75**: 1877-1883 [PMID: 8282645 DOI: 10.1152/jappl.1993.75.4.1877]
34 **Wilson TA**. Design of the bronchial tree. *Nature* 1967; **213**: 668-669 [PMID: 6031769 DOI: 10.1038/213668a0]
35 **Al Mukahal FHH**, Duffy BR, Wilson SK. Advection and Taylor-Aris dispersion in rivulet flow. *Proc Math Phys Eng Sci* 2017; **473**: 20170524 [PMID: 29225503 DOI: 10.1098/rspa.2017.0524]
36 **Berezhkovskii AM**, Skvortsov AT. Aris-Taylor dispersion with drift and diffusion of particles on the tube wall. *J Chem Phys* 2013; **139**: 084101 [PMID: 24006968 DOI: 10.1063/1.4818733]
37 **Scherer PW**, Shendalman LH, Greene NM, Bouhuys A. Measurement of axial diffusivities in a model of the bronchial airways. *J Appl Physiol* 1975; **38**: 719-723 [PMID: 1141102 DOI: 10.1152/jappl.1975.38.4.719]
38 **Fredberg JJ**. Augmented diffusion in the airways can support pulmonary gas exchange. *J Appl Physiol Respir Environ Exerc Physiol* 1980; **49**: 232-238 [PMID: 7400006 DOI: 10.1152/jappl.1980.49.2.232]
39 **Lacquet LM**, Van Der Linden LP, Paiva M. Transport of H_2 and SF_6 in the lung. *Respir Physiol* 1975; **25**: 157-173 [PMID: 1202597 DOI: 10.1016/0034-5687(75)90094-8]
40 **Chang DB**, Lewis SM, Young AC. A theoretical discussion of diffusion and convection in the lung. *Math Biosci* 1976; **29**: 331-349 [DOI: 10.1016/0025-5564(76)90110-3]
41 **Pack A**, Hooper MB, Nixon W, Taylor JC. A computational model of pulmonary gas transport incorporating effective diffusion. *Respir Physiol* 1977; **29**: 101-123 [PMID: 847307 DOI: 10.1016/0034-5687(77)90121-9]
42 **Worth H**, Adaro F, Piiper J. Penetration of inhaled He and SF_6 into alveolar space at low tidal volumes. *J Appl Physiol Respir Environ Exerc Physiol* 1977; **43**: 403-408 [PMID: 199565 DOI: 10.1152/jappl.1977.43.3.403]
43 **Nixon W**, Pack A. Effect of altered gas diffusivity on alveolar gas exchange-a theoretical study. *J Appl Physiol Respir Environ Exerc Physiol* 1980; **48**: 147-153 [PMID: 7353967 DOI: 10.1152/jappl.1980.48.1.147]
44 **Cumming G**, Horsfield K, Preston SB. Diffusion equilibrium in the lungs examined by nodal analysis. *Respir Physiol* 1971; **12**: 329-345 [PMID: 5136022 DOI: 10.1016/0034-5687(71)90074-0]
45 **Scherer PW**, Shendalman LH, Greene NM. Simultaneous diffusion and convection in single breath lung washout. *Bull Math Biophys* 1972; **34**: 393-412 [PMID: 4657076 DOI: 10.1007/BF02476450]
46 **Paiva M**. Gas transport in the human lung. *J Appl Physiol* 1973; **35**: 401-410 [PMID: 4732334 DOI: 10.1152/jappl.1973.35.3.401]
47 **Chang HK**, Cheng RT, Farhi LE. A model study of gas diffusion in alveolar sacs. *Respir Physiol* 1973; **18**: 386-397 [PMID: 4746962 DOI: 10.1016/0034-5687(73)90100-X]
48 **Davidson MR**, Fitz-Gerald JM. Transport of O_2 along a model pathway through the respiratory region of the lung. *Bull Math Biol* 1974; **36**: 275-303 [PMID: 4424249 DOI: 10.1007/BF02461329]
49 **Davidson MR**. Lung gas mixing during expiration following an inspiration of air. *Bull Math Biol* 1975; **37**: 113-126 [PMID: 1156692 DOI: 10.1007/BF02470618]
50 **Davidson MR**. The influence of gas exchange on lung gas concentrations during air breathing. *Bull Math Biol* 1977; **39**: 73-86 [PMID: 830193 DOI: 10.1007/BF02460682]
51 **Paiva M**, Engel LA. The anatomical basis for the sloping N_2 plateau. *Respir Physiol* 1981; **44**: 325-337 [PMID: 7268221 DOI: 10.1016/0034-5687(81)90027-X]
52 **Kety SS**. The theory and applications of the exchange of inert gas at the lungs and tissues. *Pharmacol Rev* 1951; **3**: 1-41 [PMID: 14833874 DOI: 10.1007/BF02432785]
53 **Farhi LE**. Elimination of inert gas by the lung. *Respir Physiol* 1967; **3**: 1-11 [PMID: 6059100 DOI: 10.1016/0034-5687(67)90018-7]
54 **Yamaguchi K**, Okada Y. Multi-compartment analysis on ventilation-perfusion inequality in the lungs studied by multiple inert gas washout. *Kokyu* 1985; **4**: 1455-1466
55 **Piiper J**, Dejours P, Haab P, Rahn H. Concepts and basic quantities in gas exchange physiology. *Respir*

Physiol 1971; **13**: 292-304 [PMID: 5158848 DOI: 10.1016/0034-5687(71)90034-X]
56 **Wagner PD**, Saltzman HA, West JB. Measurement of continuous distributions of ventilation-perfusion ratios: theory. *J Appl Physiol* 1974; **36**: 588-599 [PMID: 4826323 DOI: 10.1152/jappl.1974.36.5.588]
57 **Wagner PD**, Laravuso RB, Uhl RR, West JB. Continuous distributions of ventilation-perfusion ratios in normal subjects breathing air and 100 per cent O_2. *J Clin Invest* 1974; **54**: 54-68 [PMID: 4601004 DOI: 10.1172/JCI107750]
58 **Wagner PD**, West JB, JB West. Ventilation-perfusion relationships. In: JB West. Pulmonary Gas Exchange. JB West. New York: Academic Press 1980; 219-262
59 **West JB**, Wagner PD, RG Crystal, PJ Barns, JB West, ER Weibel. Ventilation-perfusion relationships. In: RG Crystal, PJ Barns, JB West, ER Weibel. The LUNG Scientific Foundations (second edition). RG Crystal, PJ Barns, JB West, ER Weibel. Philadelphia: Lippincott-Raven Publishers 1997; 1693-1709
60 **Bidani A**, Flumerfelt RW, Crandall ED. Analysis of the effects of pulsatile capillary blood flow and volume on gas exchange. *Respir Physiol* 1978; **35**: 27-42 [PMID: 734248 DOI: 10.1016/0034-5687(78)90038-5]
61 **Yamaguchi K**. O_2-CO_2 diagram and its physiological significance. *Kokyu* 1985; **4**: 405-414
62 **Briscoe WA**. A method for dealing with data concerning uneven ventilation of the lung and its effects on blood gas transfer. *J Appl Physiol* 1959; **14**: 291-298 [PMID: 13654151 DOI: 10.1152/jappl.1959.14.3.291]
63 **Young IH**, Wagner PD. Effect of intrapulmonary hematocrit maldistribution on O_2, CO_2, and inert gas exchange. *J Appl Physiol Respir Environ Exerc Physiol* 1979; **46**: 240-248 [PMID: 217855 DOI: 10.1152/jappl.1979.46.2.240]
64 **Yamaguchi K**, Mori M, Kawai A, Asano K, Takasugi T, Umeda A, Kawashiro T, Yokoyama T. Effects of pH and SO_2 on solubility coefficients of inert gases in human whole blood. *J Appl Physiol* 1993; **74**: 643-649 [PMID: 8458779 DOI: 10.1152/jappl.1993.74.2.643]
65 **Yamaguchi K**, Tsuji T, Aoshiba K, Nakamura H. Simultaneous measurement of pulmonary diffusing capacity for carbon monoxide and nitric oxide. *Respir Investig* 2018; **56**: 100-110 [PMID: 29548647 DOI: 10.1016/j.resinv.2017.12.006]
66 **Yamaguchi K**, Mori M, Kawai A, Takasugi T, Asano K, Oyamada Y, Aoki T, Fujita H, Suzuki Y, Yamasawa F. Ventilation-perfusion inequality and diffusion impairment in acutely injured lungs. *Respir Physiol* 1994; **98**: 165-177 [PMID: 7817048 DOI: 10.1016/0034-5687(94)00061-1]
67 **Wagner PD**, Naumann PF, Laravuso RB. Simultaneous measurement of eight foreign gases in blood by gas chromatography. *J Appl Physiol* 1974; **36**: 600-605 [PMID: 4151148 DOI: 10.1152/jappl.1974.36.5.600]
68 **Olszowka AJ**, Wagner PD, JB West. Pulmonary Gas Exchange. Numerical analysis of gas exchange. . JB West. Pulmonary Gas Exchange. New York: Academic Press 1980; 263-306 (chapter 8)
69 **Evans JW**. Mathematical analysis of compartmental lung models. New York: Academic Press 1980; 307-334
70 **Evans JW**, Wagner PD. Limits on V_A/Q distributions from analysis of experimental inert gas elimination. *J Appl Physiol Respir Environ Exerc Physiol* 1977; **42**: 889-898 [PMID: 195926 DOI: 10.1152/jappl.1977.42.6.889]
71 **Wagner PD**. A general approach to the evaluation of ventilation-perfusion ratios in normal and abnormal lungs. *Physiologist* 1977; **20**: 18-25 [PMID: 854533]
72 **Wagner PD**. Measurement of the distribution of ventilation-perfusion ratios. New York: Academic Press 1978; 217-260
73 **Ratner ER**, Wagner PD. Resolution of the multiple inert gas method for estimating V_A/Q maldistribution. *Respir Physiol* 1982; **49**: 293-313 [PMID: 6293027 DOI: 10.1016/0034-5687(82)90118-9]
74 **Wagner PD**, Dantzker DR, Dueck R, de Polo JL, Wasserman K, West JB. Distribution of ventilation-perfusion ratios in patients with interstitial lung disease. *Chest* 1976; **69**: 256-257 [PMID: 1248296 DOI: 10.1378/chest.69.2_Supplement.256]
75 **Wagner PD**, Dantzker DR, Dueck R, Clausen JL, West JB. Ventilation-perfusion inequality in chronic obstructive pulmonary disease. *J Clin Invest* 1977; **59**: 203-216 [PMID: 833271 DOI: 10.1172/JCI108630]
76 **Wagner PD**. Ventilation-perfusion inequality and gas exchange during exercise in lung disease. Madison Wisconsin: The University of Wisconsin Press 1977; 345-356
77 **Piiper J**. Variations of ventilation and diffusing capacity to perfusion determining the alveolar-arterial O_2 difference: theory. *J Appl Physiol* 1961; **16**: 507-510 [PMID: 13735693 DOI: 10.1152/jappl.1961.16.3.507]
78 **Yamaguchi K**, Kawai A, Mori M, Asano K, Takasugi T, Umeda A, Yokoyama T. Continuous distributions of ventilation and gas conductance to perfusion in the lungs. *Adv Exp Med Biol* 1990; **277**: 625-636 [PMID: 1965763 DOI: 10.1007/978-1-4684-8181-5_71]
79 **Yamaguchi K**, Kawai A, Mori M, Asano K, Takasugi T, Umeda A, Kawashiro T, Yokoyama T. Distribution of ventilation and of diffusing capacity to perfusion in the lung. *Respir Physiol* 1991; **86**: 171-187 [PMID: 1780598 DOI: 10.1016/0034-5687(91)90079-X]
80 **Yamaguchi K**, Mori M, Kawai A, Takasugi T, Oyamada Y, Koda E. Inhomogeneities of ventilation and the diffusing capacity to perfusion in various chronic lung diseases. *Am J Respir Crit Care Med* 1997; **156**: 86-93 [PMID: 9230730 DOI: 10.1164/ajrccm.156.1.9607090]
81 **Krogh A**, Lindhard J. The volume of the dead space in breathing and the mixing of gases in the lungs of man. *J Physiol* 1917; **51**: 59-90 [PMID: 16993378 DOI: 10.1113/jphysiol.1917.sp001785]
82 **Haldane JS**. A British Medical Association Lecture on some recent advances in the physiology of respiration, renal secretion, and circulation. *Br Med J* 1921; **1**: 409-413 [PMID: 20770221 DOI: 10.1136/bmj.1.3142.409]
83 **Fenn WO**, Rahn H, Otis AB. A theoretical study of the composition of the alveolar air at altitude. *Am J Physiol* 1946; **146**: 637-653 [PMID: 20996488 DOI: 10.1152/ajplegacy.1946.146.5.637]
84 **Riley RL**, Cournand A. Ideal alveolar air and the analysis of ventilation-perfusion relationships in the lungs. *J Appl Physiol* 1949; **1**: 825-847 [PMID: 18145478 DOI: 10.1152/jappl.1949.1.12.825]
85 **Rahn H**. A concept of mean alveolar air and the ventilation-blood flow relationships during pulmonary gas exchange. *Am J Physiol* 1949; **158**: 21-30 [PMID: 18133090 DOI: 10.1152/ajplegacy.1949.158.1.21]
86 **Riley RL**, Lilienthal JL. On the determination of the physiologically effective pressures of oxygen and carbon dioxide in alveolar air. *Am J Physiol* 1946; **147**: 191-198 [PMID: 21000736 DOI: 10.1152/ajplegacy.1946.147.1.191]
87 **Rahn H**, Fenn WO. A Graphical Analysis of the Respiratory Gas Exchange. Washington DC: The American Physiological Society 1955; 1-41

88 **Guenard H**, Varene N, Vaida P. Determination of lung capillary blood volume and membrane diffusing capacity in man by the measurements of NO and CO transfer. *Respir Physiol* 1987; **70**: 113-120 [PMID: 3659606 DOI: 10.1016/S0034-5687(87)80036-1]

89 **Borland CD**, Higenbottam TW. A simultaneous single breath measurement of pulmonary diffusing capacity with nitric oxide and carbon monoxide. *Eur Respir J* 1989; **2**: 56-63 [PMID: 2707403]

90 **Krogh M**. The diffusion of gases through the lungs of man. *J Physiol* 1915; **49**: 271-300 [PMID: 16993296 DOI: 10.1113/jphysiol.1915.sp001710]

91 **Blakemore WS**, Forster RE, Morton JW, Ogilvie CM. A standardized breath holding technique for the clinical measurement of the diffusing capacity of the lung for carbon monoxide. *J Clin Invest* 1957; **36**: 1-17 [PMID: 13398477 DOI: 10.1172/JCI103402]

92 **Roughton FJ**, Forster RE. Relative importance of diffusion and chemical reaction rates in determining rate of exchange of gases in the human lung, with special reference to true diffusing capacity of pulmonary membrane and volume of blood in the lung capillaries. *J Appl Physiol* 1957; **11**: 290-302 [PMID: 13475180 DOI: 10.1152/jappl.1957.11.2.290]

93 **Zavorsky GS**, Hsia CC, Hughes JM, Borland CD, Guénard H, van der Lee I, Steenbruggen I, Naeije R, Cao J, Dinh-Xuan AT. Standardisation and application of the single-breath determination of nitric oxide uptake in the lung. *Eur Respir J* 2017; 49 [PMID: 28179436 DOI: 10.1183/13993003.00962-2016]

94 **Hlastala MP**. Diffusing-capacity heterogeneity. Bethesda Maryland: American Physiological Society 1987; 217-232

95 **Piiper J**, Sikand RS. Determination of D_{CO} by the single breath method in inhomogeneous lungs: theory. *Respir Physiol* 1966; **1**: 75-87 [PMID: 5912141 DOI: 10.1016/0034-5687(66)90030-2]

96 **Sikand RS**, Piiper J. Pulmonary diffusing capacity for CO in dogs by the single breath method. *Respir Physiol* 1966; **1**: 172-192 [PMID: 5911880 DOI: 10.1016/0034-5687(66)90015-6]

97 **Hughes JM**, Pride NB. Examination of the carbon monoxide diffusing capacity (D_{LCO}) in relation to its K_{CO} and V_A components. *Am J Respir Crit Care Med* 2012; **186**: 132-139 [PMID: 22538804 DOI: 10.1164/rccm.201112-2160CI]

98 **Magini A**, Apostolo A, Salvioni E, Italiano G, Veglia F, Agostoni P. Alveolar-capillary membrane diffusion measurement by nitric oxide inhalation in heart failure. *Eur J Prev Cardiol* 2015; **22**: 206-212 [PMID: 24165475 DOI: 10.1177/2047487313510397]

99 **Zavorsky GS**, Borland C. Confusion in reporting pulmonary diffusing capacity for nitric oxide and the alveolar-capillary membrane conductance for nitric oxide. *Eur J Prev Cardiol* 2015; **22**: 312-313 [PMID: 24676716 DOI: 10.1177/2047487314528872]

100 **Austrian R**, Mcclement JH, Renzetti AD, Donald KW, Riley RL, Cournand A. Clinical and physiologic features of some types of pulmonary diseases with impairment of alveolar-capillary diffusion; the syndrome of "alveolar-capillary block". *Am J Med* 1951; **11**: 667-685 [PMID: 14902838 DOI: 10.1016/0002-9343(51)90019-8]

101 **West JB**. Restrictive diseases. Baltimore: Williams Wilkins 1982; 92-111

102 **Forster RE II**, DuBois AB, Briscoe WA, Fisher AB. Diffusion. The Lung Physiologic Basis of Pulmonary Function Tests (3rd edition). Chicago: Year Book Medical Publishers, Inc 1986; 190-222

P- Reviewer: Deng B

S- Editor: Cui LJ **L- Editor:** Filipodia **E- Editor:** Zhang YL

Published By Baishideng Publishing Group Inc
7901 Stoneridge Drive, Suite 501, Pleasanton, CA 94588, USA
Telephone: +1-925-2238242
Fax: +1-925-2238243
E-mail: bpgoffice@wjgnet.com
Help Desk: https://www.f6publishing.com/helpdesk
https://www.wjgnet.com